"POLITEHNICA" UNIVERSITY OF BUCHAREST
Doctoral School of Electrical Engineering

Eng. DALEA ALEXANDRU

ROTARY MAGNETOSTRICTIVE MOTOR

- PHD THESIS -

Scientific advisor
Prof. Dr. Ing. NECULAI GALAN
Bucharest
2021

CONTENTS

LIST OF ABBREVIATIONS

The study of magnetostriction involves several fundamental fields: electromagnetism, mechanics, thermodynamics, chemistry. In each of these areas there are notations devoted to the physical quantities used which sometimes overlap. As a result, the notations used were centralized in this list; in the thesis were made the necessary specifications.

H $[A/m]$ - magnetic field strength

B $[T]$ - magnetic induction

ε $[F/m]$ - environment electrical permittivity

μ $[H/m]$ - environment magnetic permeability

E $[V/m]$ - electric field intensity

D $[C/m^2]$ - the electric induction

w_m $[J/m^3]$ - magnetic energy volume density

w_e $[J/m^3]$ - electric energy volume density

m $[A \cdot m^2]$ - magnetic moment

Ψ, ϕ $[Wb]$ - magnetic flux

e $[V]$ - electromotor voltage

L $[H]$ - the coil's own inductivity

M[H]- mutual inductiveness between coils

i, I $[A]$ - electric current intensity

t $[s]$ - time

f $[Hz]$ - frequency

$\omega = 2\pi f$ $[Hz]$ - pulsation

Z $[\Omega]$ - electrical impedance

w, N [adim] - number of turns

δ $[m]$ - magnetic circuit switch

ρ $[\Omega m]$ - electrical resistivity of the conductor

R_m $[Asp/Wb]$ sau $[sp/H]$ - magnetic reluctance

M $[A/m]$ - magnetization

M_s $[A/m]$ - saturation magnetization

T[^{0}K] – absolute temperature

S[kcal/^{0}K] – system entropy

p[kg/m^2] – mechanical pressure

V[m^3] – the volume of the domain considered

1.INTRODUCTION.

Magnetostriction is of two types:
1. **Spontaneously magnetostriction** appears in material elements with magnetic properties within an alloy or a compound substance, when it is in a null external magnetic field, at temperatures lower than the Curie temperature. The element belonging to the alloy makes the transition from the state of magnetic disorder called paramagnetism to an magnetic ordered state, forming the Magnetic Weiss Domains.
2. Induced magnetostriction is the result of the orientation of magnetic domains when applying an external magnetic field. **Linear magnetostriction** occurs due to a linear magnetic field causing a magnetization at saturation of the lower value and leading to an elongation of the ferromagnetic core. If the magnetic field progressively increases to values similar to those necessary to achieve saturation, the induced magnetostriction no longer occurs, i.e. elongation no longer increases, [1,…,12].
In the present work is used the induced magnetostriction, that is, the one that is determined by the presence of the linear magnetic field oriented on one direction.

1.1. Magnetostrictive materials.

1.1.1. Terphenol.

The studies continued at the Naval Ordnance Laboratory (NOL)", currently the Naval Suface Warfare Center in maryland, U.S.A. – where the most advanced current magnetostrictive material, called TERPHENOL-D, was obtained.
Among the important magnetostrictive materials, the magnetostrictive material Terphenol-D is considered the ideal material for the manufacture of magnetostrictive motors. Terphenol-D is able to supply a magnetostriction of 1000-2000 ppm at a magnetic field strength of 50-200 kA/m. Terphenol-D exhibits the highest range of temperatures in the magnetostrictive process in relation to other known magnetostrictive materials and shows an acceptable compromise between high tensioning and high curie temperature.
The phenomenon of magnetostriction has been known for over 150 years (he discovered magnetostriction at Ni), so the applications appeared in 1963 with the discovery of giant magnetostriction at Tb (Terbium) and Dy (Dysprosium) at low temperatures, but the materials highlighted a number of disadvantages. All rare earths have Curie temperatures lower than ambient temperatures ($25 \div 30^{\circ} C$). To increase curie temperature values, rare magnetostrictive earths like Tb and Dy were alloyed with transitional magnetic metals (Ni, Fe and Co). Some compound materials show higher Curie temperatures (up to $800^{\circ} C$) thus magnetostriction to $25^{\circ} C$ has moderate values. The discovery in 1971 revealed that there are compounds that exhibit giant magnetostriction at the initial temperature of the environment. At very high values of magnetostriction, the magnetic anisotropics of the elements from which the compound is made, are very high, which leads to a magnetostriction of saturation obtained by very high magnetic fields.
Thus, high magnetostriction and low magnetic anisotropy are due to contrary sizes.
In order to obtain an alloy with advanced magnetostrictive properties, the following are required:

- The coefficients for the thermal expansion of the phases constituting thus to great differences between these constituents, then relatively high internal voltages in the

alloy are induced, which lead to its scrapping. Thus, the chemical compatibility of the matrix material with that of the dispersed phases is necessary, and for the constituent stages the elasticity modules must be similar. It is necessary to take into account the magnetic interactions between the constituent stages. At the differences between the magnetic permeabilities of the elements that form the composite, the phenomenon of interconstitutive magnetic shielding results (between the constituents that form the valid composition, a phenomenon valid in particular cases); The presence of phase two increases the density of the interdomenial retaining walls, thus decreasing the magnetic sensitivity of the composite material. The magnetic properties of an alloy are raised so a magnetic coupling is made between the constituent phases.

The maximum specific deformation is a key parameter for devices that use GMM. Compared to other GMM (Giant Magnetostrictive Materials) materials, at Terphenol-D there is compatibility between high values for specific deformation and high Curie temperature. Magnetostriction occurs at temperatures below Curie temperature, but often the Curie temperature is below ambient temperature, so the practical value of the specific deformation is small.

The available terphenol-D is an alloy of iron with terbium and dysprosium, of silver hue, very brittle at ambient temperature especially at stretching and due to the basic materials it is strongly reactive, contains impurities and is difficult to produce. Sintering processes are also used to obtain material for high frequencies ($1kHz$).

The shape of the material is bar diameter up to $65mm$, length up to $200mm$ and with square section, tubes, discs, plates.

The material is very friable when stretching. Permissible strain on stretching ($28MPa$) is very small compared to the value corresponding to compression ($880MPa$).

The density of the material is higher than the density of the usual steels; the average value is about $9250\ kg/m^3$.

In principle, in magnetostrictive actuators, the coil is wrapped around a tube in which the bar of terphenol is forcibly inserted (by compression). When an alternating current passes through the coil, the terphenol core will perform an elongation-tightening movement, thus obtaining a vibrating motor or a linear motor, [12,…,30].

The usefulness of the engines, produced by the company ETREMA, were used by the American Department of Defense to develop smart wings, which can change the area of the cross-section, improving the aerodynamic properties thus reducing fuel consumption, [14,…,16].

The applicative domains of magnetostrictive actuators are:

controlled distribution of fluids in the medical field, transports especially in the construction of sunscreen panels, braking systems, etc.

1.1.2. Galphenol

Remote microactuators are of great interest in biology and medicine as non-invasive intracellular stimulation equipment. Remote action can be achieved by active magnetostrictive transducers that are able to modify their shape in response to external magnetic fields, thus creating controlled displacements. Among magnetostrictive materials, Galphenol, the intelligent iron-based material, provides a high magnetostriction with robust mechanical properties. In order to explore these capabilities for biomedical applications, it is necessary to

study the feasibility of miniaturizing materials in standard manufacturing processes, as well as to evaluate biocompatibility.
The development of biological or biomedical microelectromechanical systems (BioMEMS) has created multifunctional tools capable of individually addressing the biochemical or mechanical processes performed by cells. In addition to their sensory properties, there has been a growing interest in the action characteristics offered by these devices through electrical, mechanical or magnetic forces. With the introduction of smart materials into these devices, it was possible to obtain an addressable external control. Of these materials, solutions for the giant magnetostriction, have emerged as effective tools to create remotely controlled deformations using external magnetic fields, to act alone or in combination with other intelligent materials in tandem to create more complex capabilities. In fact, the integration of magnetoelastic materials into the MEMS has brought a remarkable performance, since they provide "autotest, self-calibrating, remote sensing and actuation" properties, which provide the necessary system for less invasive biomedical instruments. One of the most versatile examples of huge magnetostrictive materials is Galphenol, an iron alloy capable of transmitting magnetic energy in mechanical deformation with tensions that grow up to hundreds of ppm at low-saturation magnetic fields. Mechanical force overcomes mechanical problems of its counterpart Terphenol-D which has a higher magnetostriction (~ 2000 ppm), but it is very fragile at room temperature. On the contrary, Galphenol has a high ductility and high tensile strength, bending and compressive forces, which are preserved at the micro and nano scale. It can also be sprinkled from a fixed target of the alloy composition, creating thin films of high quality and coherent in a composite way, with the correct proportion of gallium and iron to ensure its magnetostriction.
The versatility of this material has paved the way for several applications from micro-accumulators to micro and nanorobors. Although the introduction of Galphenol to BioMEMs is only exploratory to date, it is still necessary to ensure its biocompatibility as a first step in the development of medical applications. The first attempt to assess the biocompatibility of Galphenol was carried out by indirect cytotoxic analyses using millimetre blocks in contact with the culture medium. Once the blocks were removed, the medium was used to incubate fibroblasts without negative results in cell survival, in addition the biodegradable properties of Galphenol also proved negligible, showing prospects for the alloy in biological applications. Galphenol nanowires were also internalized by cells, showing cellular viability in a preliminary test of qualitative toxicity [14,..,19].

The objective of the thesis consists in the theoretical and experimental analysis of the efficient functioning of the rotary magnetostrictv motor. For this purpose, we started from the physical foundations of the magnetostriction phenomenon that explains the characteristic of magnetostrictive elongation – magnetic field. In order to accurately establish the values of the performance operating parameters, at high magnetic energy density, it was established the dependence of the magnetostrictive force on the magnetostrictive elongation and the phenomena that can modify the optimal operating point were highlighted. The study of this engine is completed with experimental data.

2. Explanation of the phenomenon of magnetostriction based on Magnetic Domains Weiss.

2.1. Elements concerning the structure of the atom.

To make it clearer to present the issue, we will mention some elements related to the structure of the atom.
Within quantum physics, it is believed that electrons could be in an orbital motion surrounding the nucleus, according to Niels Bohr, and it is now stated that they have multiple levels of energy, which are distinguished by four quantum numbers. The electrons that are in the electron shell, i.e. the space around the nucleus, in accordance with the available energy, are ordered at energy levels i.e. energy layers numbered ascending in accordance with the available energy level, so the number of a layer is equal to the main quantum number, n. Energy levels are divided into sublevels that contain a certain number of orbitals. Electrons move in variable orbits with different shapes around the nucleus. The type of atom characterizes the orbital that highlights the space around the nucleus that increases the possibility of finding electrons. According to Wolfgang Pauli there was no orbital containing identical electrons. To each sublevel we have attached a secondary quantum number l.
The magnetic quantum number, m, indicates the number of orbitals in a substrate and characterizes the state of electrons in magnetic fields. The electrons that revolve around the atomic nucleus represent circular currents, which, according to classical electrodynamics, are equivalent to a small magnet that are characterized by the magnetic moment. The vector resultant of the magnetic moments corresponding to all orbitals constitutes the vector of the total magnetic moment of the atom. When the outer magnetic field is absent, the direction of the magnetic moment of the atom can be some such that its energy content is not influenced. If the atom is placed in an outer magnetic field, it exerts an orientation action on the magnetic moment in relation to the disturbing magnetic field, which causes the spectral lines of that element to present a fine structure . Thus, it is necessary to introduce a quantum number for the precise knowledge of the energy state in the atoms.
Orbitals are distinguished by the volume around the atomic nucleus at which the probability of finding an electron is maximum.
Two electrons is the maximum value attributable to an orbital.
The electronic shell of the atom is structured on energy levels, which are divided into sublevels with corresponding orbitals. The sub-tiers are denoted by s (from eng.sharp), p (eng:principal), d (eng. diffus) and f (eng.fundamental).
The main quantum number, n describes the belonging of an electron to a certain energy level.
The secondary quantum number, l describes the belonging of electrons to a certain sublevel.
The magnetic quantum number, ml describes the spatial orientation of the orbitals, which identify orbitals within the substrates, and each value of ml corresponds to one of the permitted orientations for the magnetic field associated with the orbital (for a substrate "p" - ml it can be -1.0 or 1, for a substrate "d", ml can be -2,-1,-1,0,1 or 2, etc.).
The quantum spin number, ms: describes the proper rotational momentum of electrons and can have the values +1/2 or -1/2.
The main features of the quantum model of the atom are as follows:
- mathematical functions describe the atomic state;
- the way of formation of the atom is from the nucleus i.e. protons and neutrons, and the electrons are distributed around the nucleus;
- electrons occupy orbitals with different shapes, depending on the atomic type;
- energy levels are represented by multiple energy sub-levels;

- *no orbital contains electrons with the same quantum numbers.*
One of the sizes that characterizes the atoms or molecules of a substance is the magnetic moment. Substances where the magnetic moment is null are called diamagnetic substances, and substances where the magnetic moment is different from zero are called paramagnetic substances. The magnetic moment of atoms or molecules is the result of the summation of the orbital magnetic moments and of the magnetic spin moments of the electrons.
The experiences of Einstein and Haas have shown that the magnetic moment of the iron atom is given entirely by the spin moments of the electrons, the orbital magnetic moments compensating for each other. And the spin moments of the electrons of an atom are largely compensated, but there are electons whose thorns are not compensated. At an iron atom, of all its 26 electrons disposed on four energy levels, only four of the six electrons available on the 3d level have uncompetent spines.

2.2. Magnetic materials. Weiss Domains.

Materials with a spontaneous magnetization other than zero below a certain temperature are ferromagnetic and ferrimagnetic, but not every piece of iron shows at room temperature a spontaneous magnetization other than zero. The explanation was given by Weiss, who assumed that a ferromagnetic material at temperatures below the critical temperature is divided into magnetic domains (Weiss domains). In each domain, which contains a large number of atoms, the magnetic moments are parallel and result in a spontaneous magnetization different from zero. From one domain to another, the direction of spontaneous magnetization is different so that the total magnetization of the material is zero.

Magnetic domains are separated by walls called interdomenic walls [2] by which is understood the portion that includes the atomic layers that separate the magnetized domains in different directions. On an atomic scale, there can be no sudden transition from one direction of magnetization to another because such a transition would involve a large contribution of exchange energy. The change of the direction of magnetization from one domain to another is done gradually on a certain number of planes of thorns.
Thus the interdomenic wall has a finite width, which as a rule is smaller than the width of adjacent domains. Due to the fact that in the wall the magnetization vector rotates gradually, it is very difficult to give a rigorous definition of the width of the interdomenic wall (both theoretically and experimentally). One quantity that can be precisely determined is the angle of the wall φ, defined as the angle made by the vectors of magnetization of adjacent domains, measured in the centers of the respective domains. The specific way in which the magnetization vector rotates in the wall reflects the structure of the wall. The width and respectively the angle of the wall are the conditions on the border of the wall that condition this structure.
A wide variety of walls are now known. At a very thin blanket of the order of hundreds of Å (iron -nickel alloys), the rotation of magnetic moments is usually made in the plane of the wall in order not to lead to the development of important magnetostatic energies (the ratio between the surface and the volume is taken into account). This type of walls are called Néel walls. In thicker blankets you can see walls with transverse connections. In substances with high magnetic anisotropy can be the walls in the skin in which the rotation of thorns is made after several atomic planes. In some cobalt ferrites are very wide walls, called kπ walls. The most famous are the bloch walls, he was the first to analyze the nature of the transition between domains comprising multiple atomic planes, whose orientation of the magnetic moment is made progressively from one domain to another. Bloch walls are specific to Weiss domains formed to ferromagnetic materials.

At the influence of the external magnetic field, there appear indicative processes of the magnetic moments that form the Weiss domains, according to the direction of the applied magnetic field and thus result in an incipient magnetization of the material, different from zero. The ferromagnetic material presents magnetic domains that confer energy reasons, namely the ratio between exchange energy and dipolar magnetic energy, the latter being maximum. When dividing the sample into N magnetic fields, the decrease of N times of the dipole magnetic energy is produced, compared to the monodomenial case.
Magnetostriction is the phenomenon by which the dimensions (shape) of a sample are modified during the magnetization process; as a result, the process of magnetization of a ferromagnetic material will be described, [2], [3].

2.3. Thermodynamic aspects of the phenomenon of magnetostriction.

By thermodynamic system one can mean any part of the universe, for which an interior and an exterior containing a practically small number of macroscopic bodies can be established, considering that they have a continuous structure. The state of any thermodynamic system will be described by a certain group of parameters, the group being considered complete if the states of two identical thermodynamic systems, described by the same values of the parameters, cannot be distinguished from each other by experiments performed at the macroscopic scale, [42 ... 45].
The action of a parameter A generally results in a variation of a parameter *a*. For the group of mechanical parameters to be complete, it is necessary that each force parameter A corresponds to a certain position parameter *a*, that is, the number of force parameters to be equal to the number of position parameters. It is adopted that the physical dimensions of these parameters are taken in such a way that the product $A \cdot da$ represent the elementary work, i.e. $\delta L = A \cdot da$.
In the magnetic field the relationship between **B** magnetic induction, $\mathbf{I}=\mu_0\mathbf{M}$ (M is magnetization) magnetic polarization and **H** magnetic field strength is in the form of:

$$\vec{B} = \mu_0 \vec{H} + \vec{I} = \mu_0 \vec{H} + \overrightarrow{\mu_0 M} \qquad (2.1)$$

Variation in the volume density of magnetic field energy for homogeneous bodies (the **H** and **B** vectors are collinears) is:

$$d\, w_m = \vec{H}\, d\vec{B} = H\ d\left(\mu_0 H + I\right) = d\left(\mu_0 \frac{H^2}{2}\right) + H\ dI = d\ w_{mp} + d\ w_{mL}\ ; \qquad (2.2)$$

$$w_{mp} = \mu_0 \frac{H^2}{2}; \quad w_{mL} = H\ dI$$

In relation (2.2) the size w_{mp} is the own energy of the electric field in vacuum and does not produce mechanical work; w_{mL} is the energy that produces the mechanical work due to the presence in the magnetic field of the body with the I magnetic polarization, in fact, it represents the mechanical work on the unit of volume of the body with magnetic polarization.
For volume deformable bodies V, with magnetic anisotropic (the **H** and **B** vectors they are not collinears), the mechanical work of magnetic forces on the unit of volume is:

$$\vec{H}\, d\vec{I} = H_e\, dI_x + H_y\, dI_y + H_z\, dI_z \qquad (2.3)$$

Based on the relations in thermodynamics and following some calculations, the relationships are established:

$$\frac{\partial F}{\partial H} = p \frac{\partial V}{\partial H} + I \qquad (2.6)$$

In the relationship (2.6) the term is highlighted:

$$\frac{\partial V}{\partial H}=\left(\frac{\partial V}{\partial H}\right)_{p,T}=\frac{1}{p}\left(\frac{\partial F}{\partial H}\right)_{p,T}-\frac{I}{p} \qquad (2.7)$$

which represents the phenomenon of magnetostriction; that is, the variation in volume of the magnetic substance caused by the H magnetic field. This variation in volume is based on the modification of the F free energy produced by the variation of the H magnetic field.

3. THE STRUCTURE OF THE ROTARY MAGNETOSTRICTIVE MOTOR

Magnetostrictive motors can be vibrating motors, linear motors, rotary motors; whatever type of motor, the actuator used has in principle the same construction structure.
Figure 3.1 shows the main constructive elements of the rotating magnetostrictive motor, which consists of the actuator and a movable part consisting of a disc fixed on a vertical axis guided by two bearings.

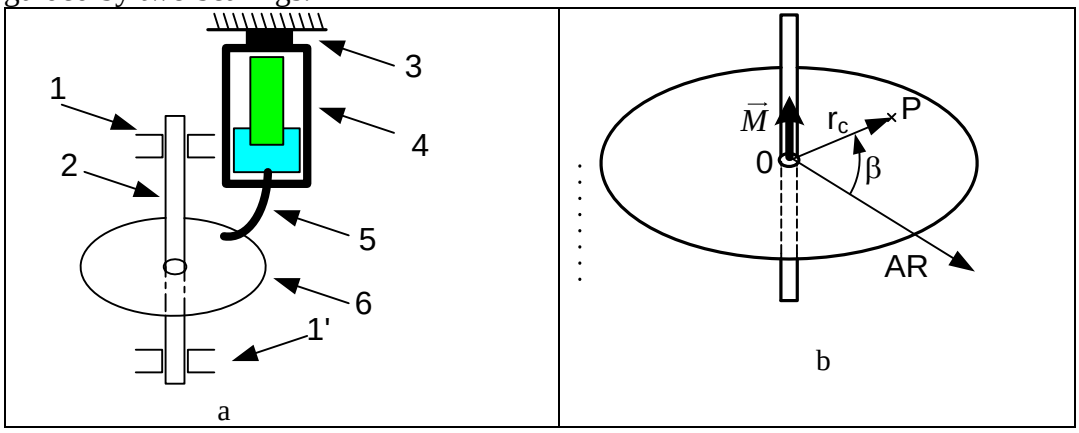

Fig. 3.1. a) Sketch of the rotary magnetostrictive motor: 1 și 1' – bearings, 2 – axle, 3 – fixing support, 4 –actuator, 5– friction element, 6 – rotor ; b) rotor disc: P – the point of contact between the disc and the friction element, r_c - the radius of the circle on which the contact point is located P, β - point angle of position P, M- torque exerted on the rotor, AR – axis of reference.

For a high performance operation, the permanent magnet must achieve in the terphenol rod a H_A magnetic field corresponding to the A point, (fig. 2.8), on feature $\lambda = f(H)$.
Using also the demagnetization characteristic of the permanent magnet, the procedure for achieving these requirements and the experimental verification module will be analyzed, [60].

3.1. Magnetic circuit equivalent diagram.

3.1.1. The permanent magnet.

In the operation of the actuator it is of interest to establish the operating point in order to assess the influence of the magnet on the performances of the actuator. A permanent magnet is defined by its demagnetization characteristic (experimentally high) and its geometry; a first

problem is to associate an equivalent magnetic circuit with a permanent magnet, [50;51; 61; 63].
The demagnetization feature is represented in the *B-H* plane in the *II* dial ($B \geq 0, H \leq 0$) and is characterized by sizes B_r – remaining magnetic induction and H_c- coercive magnetic field strength, (fig. 3.2).

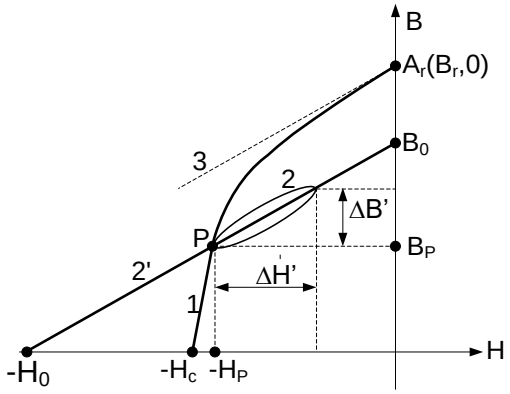

Fig. 3.2. a) Definition of the return right: 1 – demagnetization curve; 2 – return curve; 2'- right return; 3 – right tangent to the point A_r.

If the permanent actuator magnet has the P operating point, then to a change in the magnetic state of the permanent magnet (a variation of the B induction) P point no longer follows feature 1 but moves on curve 2 (a narrow hysteresis cycle) which is approximated to the 2' line called the return line. The return right is characterized by the cuts with the coordinate axes, namely the sizes $-H_0$ şi B_0.
One can calculate the solenation sizes Θ_0 and the reluctance R_m:

$$\Theta_m = H_0 L_m \; ; \quad R_m = \frac{L_m}{\mu_m S_m} \qquad (3.1)$$

where the notations in figures 3.2 and 3.4 were used.
For the analysis of the actuator's operation it is necessary to know the equivalent magnetic scheme of the magnetic circuit in which the permanent magnet is inserted. The structure of the magnetic circuit comprises several elements (sections) that are characterized by magnetic reluctance, which must be calculated with sufficient precision because it intervenes in establishing the performances of the actuator and therefore of the magnetostrictive motor.

3.1.2. Permanent magnet under the action of an outer magnetic field.

If the Θ_d = wi coil magnetization solenation is applied, then the position of the operating point changes; of the law of the magnetic circuit, applied on a closed Γ curve (fig. 3.4), it is obtained:

$$(1): \int_\Gamma \overline{H}\,\vec{dl} = H L_m + \sum_{i=1}^{i=n} V_{mi} = -\Theta_d \Rightarrow H = -\frac{\Theta_d}{L_m} - \frac{\sum_{i=1}^{i=n} V_{mi}}{L_m}. \quad (2): H = -\frac{\Theta_d}{L_m} - \frac{S_m}{k_\sigma \Lambda_e L_m} B \qquad (3.2)$$

where ΣV_{mi} represents the sum of the magnetic voltages for the n homogeneous sections of the magnetic circuit, except for the permanent magnet; each term of the amount ΣV_{mi} is a function of magnetic induction in the material of the considered section and implicitly of the induction of the permanent magnet *B*.

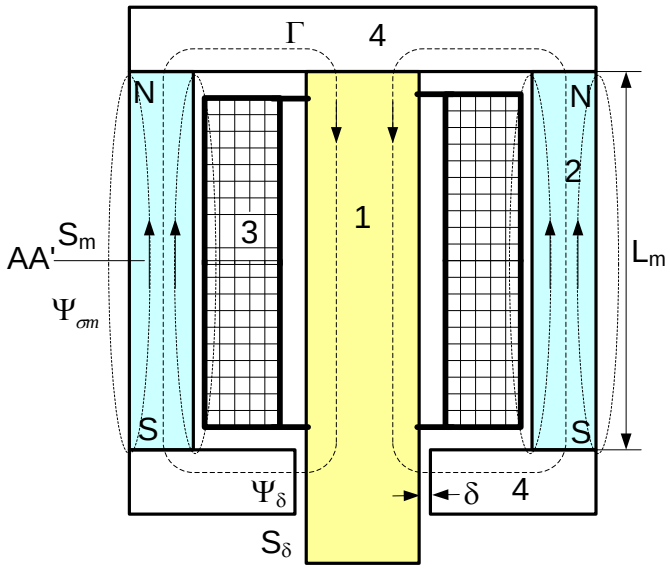

Fig. 3.4. Magnetic circuit of the actuator: 1- terphenol rod; 2 – permanent magnet; 3 – coil; 4 – ferromagnetic flanges.

3.1.3. The permeanţele of the magnetic circuit.

Consider the magnetic circuit in figure 3.4 and proceed to the calculation of the reluctance of each section of its composition, [62,…,64].
There are sections that present the phenomenon of hysteresis and therefore there are losses of power P_H due to this phenomenon plus power losses through swip currents P_T forming entirely the losses in iron, $P_{Fe} = P_H+P_T$. As a result, a complex reluctance will be calculated to include these power losses; at high frequencies, this component cannot be neglected.
It is considered a section of the magnetic circuit, which has losses in iron (fig. 3.6) for which clarifications are made regarding the phenomenon of hysteresis.

It is assumed that the variation of the B(t) induction is sinusoidal; in this case, due to the hysteresis phenomenon, the variation in the size of H(t) is no longer sinusoidal but can be decomposed into Fourier series and the fundamental is retained (harmonica 1), $H_1(t)$. The curve of the size H(t) is phased in advance to the magnetic induction curve B(t). Sinusoidal variations of sizes $B_1(t)$ and $H_1(t)$ have indices 1 and are phased in time with the angle γ_1, in other words:

$$H_1 = H_1(t) = H_{m1}\sin\omega t\ ;$$

$$B_1 = B_1(t) = B_{m1}\sin(\omega t-\gamma_1) = B_{m1}\cos\gamma_1\ \sin\omega t - B_{m1}\sin\gamma_1\cos\omega t =$$

$$= B_1^{'} + B_1^{''} = B_{m1}^{'}\sin\omega t + B_{m1}^{''}\cos\omega t\ ;\quad B_{m1}^{'} = B_{m1}\cos\gamma_1\ ;\quad B_{m1}^{''} = -B_{m1}\sin\gamma_1 \qquad (3.3)$$

$$\mu = \frac{B_{m1}}{H_{m1}}\ ;\quad \mu' = \mu_0^{'}\mu_r^{'} = \frac{B_{m1}^{'}}{H_{m1}} = \mu\cos\gamma_1\ ;\quad \mu^{''} = \mu_0^{''}\mu_r^{''} = \frac{B_{m1}^{''}}{H_{m1}} = \mu\sin\gamma_1\ ;\quad \frac{\mu^{''}}{\mu'} = tg\gamma_1$$

Sinusoidal sizes B_1 and H_1 can be expressed in an unsimplified complex in which case the complex magnetic permeability is defined $\underline{\mu}$, namely:

$$\underline{H}_1 = H_{m1}e^{j\omega t}\ ;\quad \underline{B}_1 = B_{m1}e^{j(\omega t-\gamma_1)} \Rightarrow \underline{\mu} = \frac{\underline{B}_1}{\underline{H}_1} = \mu e^{-j\gamma_1} = \mu' - j\mu^{''} \qquad (3.4)$$

We remove t parameter from the relationships (3.3) after which it is obtained:

$$H_1 = H_{m1}\sin\omega t \Rightarrow \quad \sin\omega t = \frac{H_1}{H_{m1}}$$

$$B_1 = B_1^{'} + B_1^{''} = B_{m1}^{'}\sin\omega t + B_{m1}^{''}\cos\omega t \ ;$$

$$B_1 = B_{m1}^{'}\sin\omega t + B_{m1}^{''}\cos\omega t = \mu^{'}H_{m1}\frac{H_1}{H_{m1}} \pm \mu^{''}H_{m1}\sqrt{1-\left(\frac{H_1}{H_{m1}}\right)^2} \quad (3.5)$$

$$\Rightarrow B_1 = \mu^{'}H_1 \pm \mu^{''}\sqrt{H_{m1}^2 - H_1^2}$$

The last expression in (3.5) shows that the hysteresis cycle of a material can be broken down into two components: a component B'$_1$ and a component B''$_1$, that have the expressions:

$$B_1^{'} = \mu^{'}H_1 \ ; \quad B_1^{''} = \pm\mu^{''}\sqrt{H_{m1}^2 - H_1^2} \qquad (3.6)$$

B'$_1$ component corresponds to reversible magnetization processes, and B"$_1$ component corresponds to irreversible magnetization processes and represents an ellipse whose axes coincide with the coordinate axes (fig.3.7); of (3.6) results for B''$_1$ ellipse expresion.

$$B_1^{''} = \pm\mu''\sqrt{H_{m1}^2 - H_1^2} \Rightarrow \left(\frac{H_1}{H_{m1}}\right)^2 + \left(\frac{B_1^{''}}{\mu^{''}H_{m1}}\right)^2 = 1 \qquad (3.7)$$

$$tg\alpha' = \mu_r^{'} \ ; \quad tg\alpha'' = \mu_r^{''}$$

From the relationships (3.7) results the geometric significance of the permeabilities μ_r'si $\mu_r^{"}$. (fig.3.7).

This ellipse interersects each axis of coordinates at two points (fig.3.7); goes a straight D through the abscissa point - H_{m1} and the ordered point $\mu^{''} H_{m1}$, it is found that $\mu^{''}$ is the angular coefficient of this straight.

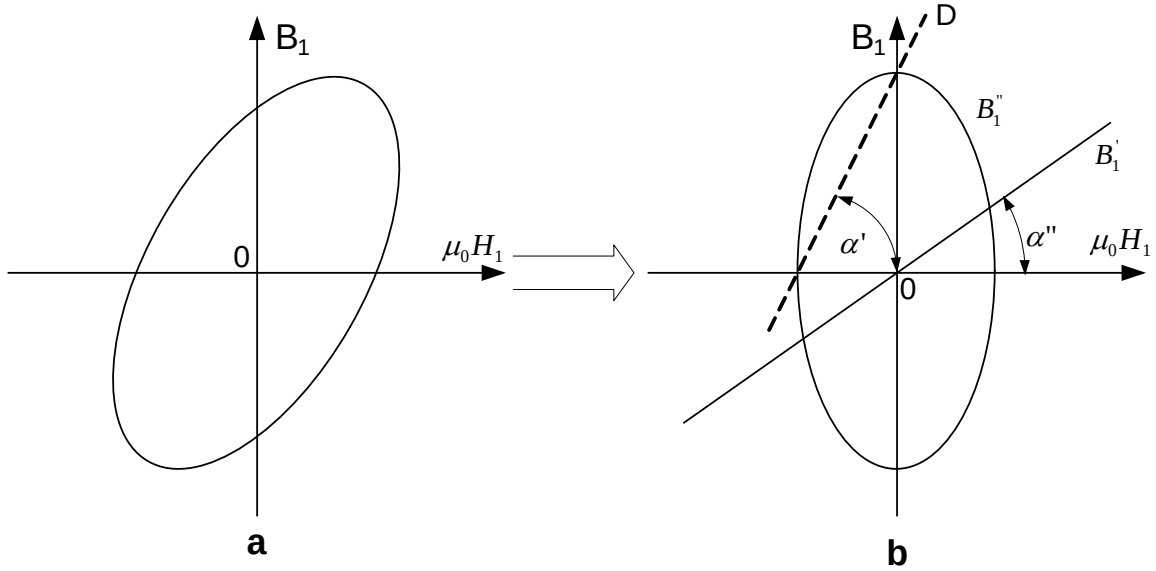

Fig. 3.7 The cycle of elliptical hysteresis (a) with its components (b) ; the significance of complex magnetic permeability components.

Losses through hysteresis per unit of volume at frequency f au expression:

$$p_{Hi} = \pi\, f\, H_{m1i}B_{m1i}\sin\gamma_1 \qquad (3.8)$$

it was considered the hysteresis curve in the shape of an ellipse.
Based on the above, the components of the complex magnetic reluctance of a portion i of a magnetic circuit, which presents the phenomenon of hysteresis, are calculated. The complex reluctance of the i portion of the magnetic circuit has the expression:

$$\underline{R}_M = R_c + j\,R_d = \frac{l_i}{S_i\,\underline{\mu}} = \frac{l_i}{S_i\,\mu^2}\left(\mu' + j\,\mu''\right)$$

$$\Rightarrow \begin{cases} R_c = \dfrac{l_i\mu'}{S_i\,\mu^2} = \dfrac{l_i\mu' H_{m1}}{H_{m1} S_i\,\mu^2} = \dfrac{N_i I_i}{\Phi_i}\cos\gamma_1\,; \quad \Phi_i = H_{m1} S_i\,\mu\,; \quad l_i H_{m1} = N_i I_i \\ R_d = \dfrac{l_i\mu''}{S_i\,\mu^2}\dfrac{\pi\,f\,H_{m1}B_{m1}\sin\gamma_1}{\pi\,f\,H_{m1i}B_{m1}\sin\gamma_1}\dfrac{S_i\,l_i}{S_i\,l_i} = \dfrac{l_i\mu''}{S_i\,\mu^2}\dfrac{P_H}{(S_i\,l_i)\pi\,f\,H_{m1}B_{m1}\sin\gamma_1} = \\ = \dfrac{2P_{Hi}}{\omega\Phi_i^2} = \dfrac{2\,P_H}{\omega\Phi_i^2} = \dfrac{2\dfrac{P_H}{G_{fi}}G_{fi}}{\omega\Phi_i^2} = \dfrac{2\,p_H G_{fi}}{\omega\Phi_i^2}\,; \quad p_{Hi} = \dfrac{P_{Hi}}{G_{fi}} \end{cases} \qquad (3.9)$$

For ferromagnetic materials with negligible iron losses $\sin\gamma_1 = 1$,
As a result of the decomposition of the hysteresis cycle, the names can be used: R_c – conservative reluctance, R_d – dissipative reluctance.
The term of magnetic reaction or inductive reaction used in the literature for dissipative reluctance R_d does not correspond to the physical significance of this size [,43; 76; 77] .
For the technical calculation of the R_d dissipative reluctance it is considered total iron losses because losses by hysteresis usually predominate. R_e equivalent reluctance of the magnetic circuit must be calculated as accurately as possible. By the load characteristic, the operating point of the permanent magnet is determined, [29; 51...54].
The equivalent magnetic scheme for a magnetic circuit with a permanent magnet is shown in figure 3.8 and is useful for establishing the operating point of the magnet. The computational relationships of conservative magnetic reluctance are:

$$R_{mc} = \frac{L_m}{\mu_m S_m}\,; \quad R_{Tc} = \frac{L_T}{\mu_T S_T}\,; \quad R_{m\sigma} = \frac{L_m}{\mu_m\pi\left(r_2^2 - r_1^2\right)}\,;$$
$$R_{Fc} = \frac{\ln\left(r_2 / r_1\right)}{2\mu_F\pi\,H_F}\,; \quad R_\delta = \frac{\delta}{2\pi\,r_1 H_F} \qquad (3.10)$$

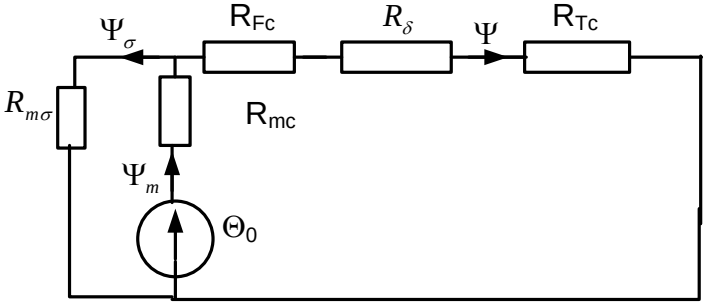

Fig. 3.8. Equivalent scheme of magnetic circuit with permanent magnet.

where L_T and L_{mp} is the average length of the field line in the magnetostrictive bar, respectively in the permanent magnet, respectively A_T and A_m are the designated areas of

cross-sections, H_F - flange thickness, r_2, r_1 - the outer and inner radius of the flange respectively, δ is the switch.

3.2. Establishing the operating point of the permanent magnet and calculating the coil sole.

a. Choosing the shape of the permanent magnet demagnetization feature.
The analysis of the positioning of the operating point, denoted A, of the permanent magnet allows to establish the optimal shape of the demagnetization characteristic. Point A on the demagnetization curve or on the return line, characterized by the intensity of the magnetic field H_A, it must not be significantly influenced by the outer fields in which the magnet is located after their disappearance.
$|H_c|$ coercive magnetic field it has to have a high value. Otherwise, when the magnet is in large outer magnetic fields, the return curve may be changed and the operating point changes its position to a significantly lower induction (point P5 in figure 3.3). The reduction of the magnetic induction in the upper area of the curve must differ slightly in relation to the remaining B_r induction (ideally it should be a slightly inclined drea to the abscissa); in this case the right return would be very close to the curve and induction for the B_A operating point would be close to B_r value ($B_A < B_r$). Magnets with linear demagnetization characteristic (fig. 3.5) would correspond to these requirements but have low B_r values for. The ideal solution would be the magnet with the demagnetization feature close to a rectangle.

b. H_{Am} magnetic field correlation of the operating point of the permanent magnet (fig. 3.10.a) with the magnetic field H_A of the elongation feature – magnetic field, (fig. 3.10.b).
It is considered that the variation in time of the current i is sinusoidal, (fig. 3.10.c). If $H_{Am} = H_A$, then λ size has a symmetrical pulsating variation,(fig. 3.10 d); this is the ideal case when λ has the maximum possible variation. In the other two cases, fig.3.10.e and fig. 3.10 f, size variation λ is diminished and the variation over time is deformed, one of the two pulses of the sinusoid is of lower amplitude. Variation in elongation over time λ tracks the variation in time of the current i in the coil, [62, 63].

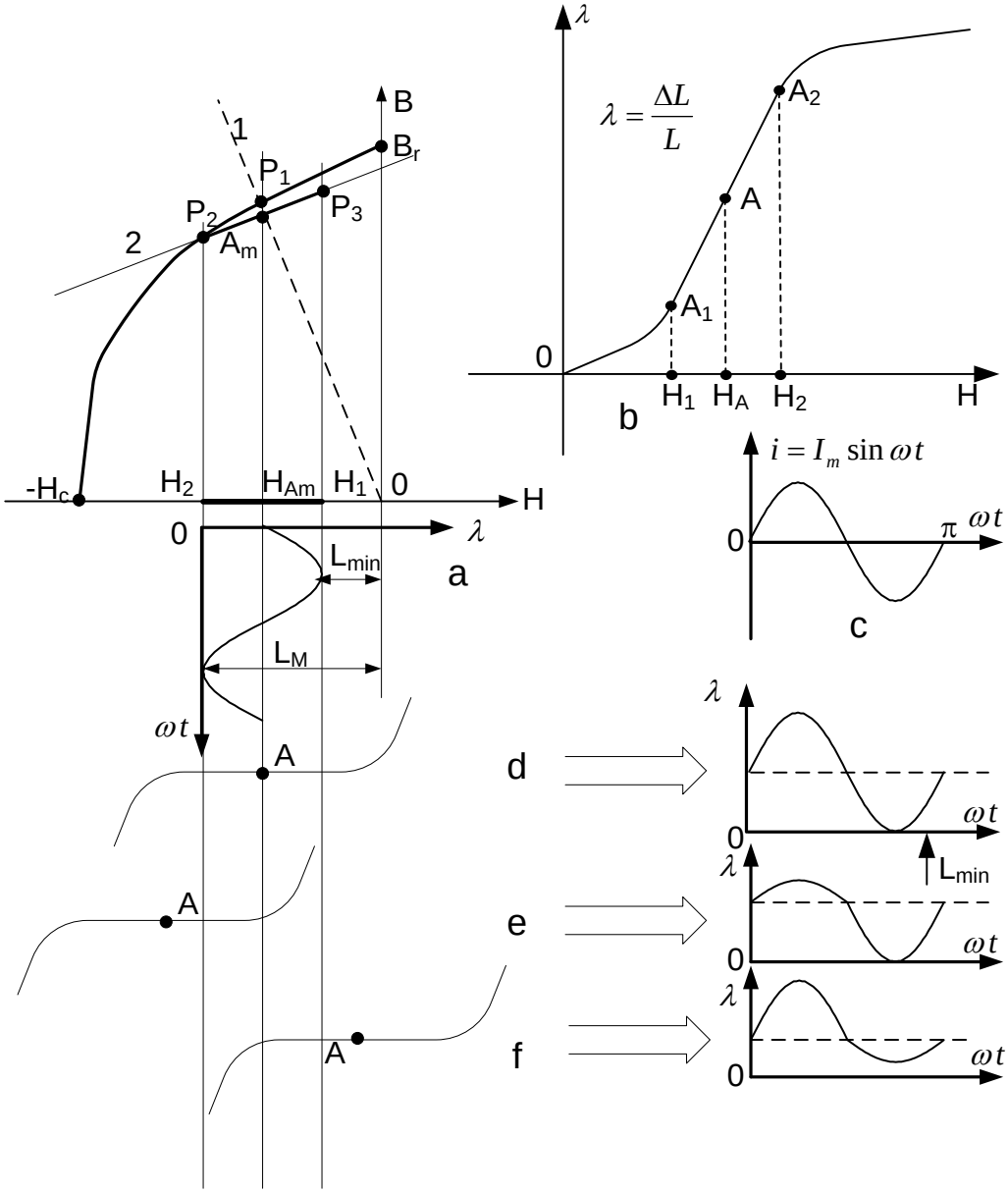

Fig. 3.10. Correlation of magnetic field intensities H_{Am} and H_A: a) Variants of positioning of points A_m andA; b) elongation-field characteristic of the magnetostrictive material; c) variation in time of current i in the coil; d) size variation λ depending on the time when H_{Am} and H_A have equal values; e) size variation λ depending on the time when $H_{Am} > H_A$; f) size variation λ depending on the time when $H_{Am} < H_A$.

In the area of the linear portion of the elongation-magnetic field character, the current in the coil has significantly lower values than in the saturated area, which is advantageous for the dimensioning of the coil and therefore the linear area must be used in the operation of the actuator.

c. Method for experimental determination of the coincidence of points A_m and A.

The three situations (fig. 3.10..d,e,f) suggest a method to experimentally determine the coincidence of the A_m and A points by recording the variation in time of the size λ and the analysis of the forms of variation in time of this quantity according to Figure 3.10. When the negative alternation (in relation to the polarity of the field produced by the permanent magnet) has a lower amplitude in relation to the positive alternation, then $H_A < H_{Am}$. When the positive alternation has the lower amplitude in relation to the negative alternation, then $H_A > H_{Am}$. The ideal solution would be the size H_{Am} coincide with the size H_A. Equality between sizes H_{Am}

and H_A it could be done with a small adjustable interfier between a flange and the permanent magnet if the current had to be adjusted within certain limits but the entire linear area of the elongation-field feature could not be used.

d. Determination of the solenaţiei of the actuator coil.

Θ_d solenation of the actuator coil must provide in the magnetostrictive rod the magnetic field of amplitude $\Delta H_m = H_1 - H_{Am}$, (fig. 3.10.a). Based on the equivalent scheme (fig. 3.9) and using the second relation of (3.11), one can write the relationships:

$$\Theta_d = wi = R_e \Psi = R_e \mu_F \Delta H_m S_F \Rightarrow wI_m = R_e \mu_F \Delta H_m S_F \qquad (3.12)$$

where μ_F and S_F are the permeability and respectively the section of the bar of the magnetostrictive material; results as the product wI_m is also determined depending on the power supply and the geometric dimensions of the actuator (permanent magnet, terphenol rod) the number of turns can be established w and the maximum current value I_m. Finally, the solution is validated by the thermal calculation of the coil. The coil is made with several sockets to have the possibility to modify the Θ_d solenation, one of these sockets corresponds to the solenation in the relation (3.12).

4. Torque of the rotary magnetostrictive motor.

The transmission of the movement is carried out through the device shown in figure 4.1 in which its components are also highlighted; in the specialized literature (based on the equations of elastic forces) it is shown that the microcontactict between the friction element and the disc rotor describes a surface bounded by a microelipse, [57].

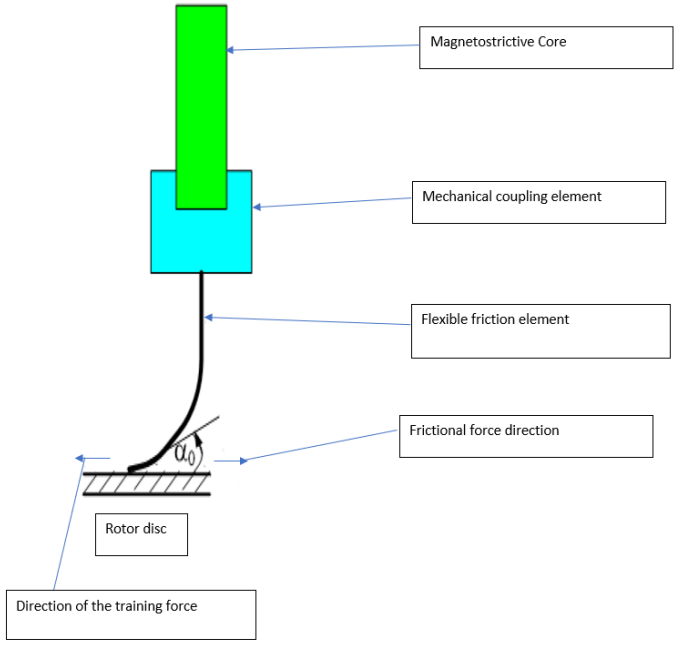

Fig. 4.1. Rotor disc and motion transmission system.

i_b current that goes through the coil and the magnetic field H_b coil product in magnetostrictive bar have the following expressions:

$$i_b = I\sqrt{2}\sin\omega t \quad \Rightarrow \quad H_b = H_{bm}\sin\omega t \qquad (4.1)$$

We consider the linear part of the magnetostriction caracracteristics (fig. 3.10.b); when the H_b field varies from the value $-H_{bm}$ at H_{bm} produced by the i_b current that goes through the coil

turns, (fig.4.2), increasing elongation ΔL takes place on the entire linear area in this way a maximum elongation is obtained and this leads to high engine performance.

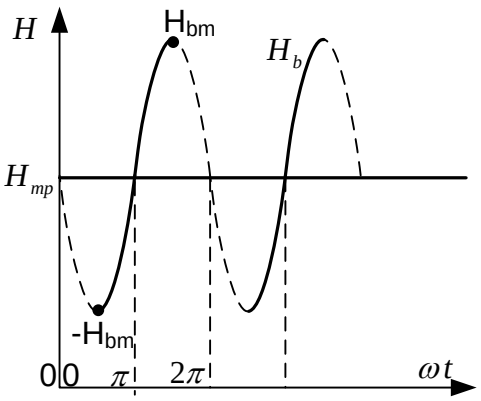

Fig. 4.2. H_b magnetic field which causes the elongation of the magneostrictive bar (the full line represents the active part for the rotor disc).

H_{mp} magnetic field is produced by the permanent magnet and must correspond to point A in figure 3.10.b.
The electromagnetic torque M acting on the disk is calculated with the relation:

$$M = F\, r_c \cos\alpha_0 = \frac{\Delta L}{\lambda_h} r_c \cos\alpha_0 \qquad (4.2)$$

where r_c is the radius from the contact point to the axis of the mobile disk, α_0 is the angle between the F force and the plane of the disk; the F force results from Hooke's law and is the driving force. [55…60] .
With the growth of the H_b magnetic field (fig. 4.2), increases and the ΔL elongation of the magnetostrictive bar and consequently increases the F force until the field reaches the H_{bm} value; according to the relationship (4.1), as a result the torque M increases, which sets in motion the rotor disc. When the H field decreases, the F force decreases (i.e. the M torque) and the friction element (fig, 4.1) weakens its adhesion to the disc (it functions as a spring), which occurs in a time interval corresponding to the very close values of the field H_b in the proximity of value H_{bm}. At the negative alternation of the H_b field, phenomena happen similiar because the function $\lambda = f(H_b)$ it is a even function and the torque M retains its meaning. The variation in time of the torque M has the period equal to that of the sinusoid in figure 4.2. On the range $[0; 7\pi/6]$ the frictional flexible element can be considered active. As is known the force F is proportional to the H_b magnetic field, and the torqueis proportional to the force F. With these specifications the torque curve M is shown as shown in figure 4.3.

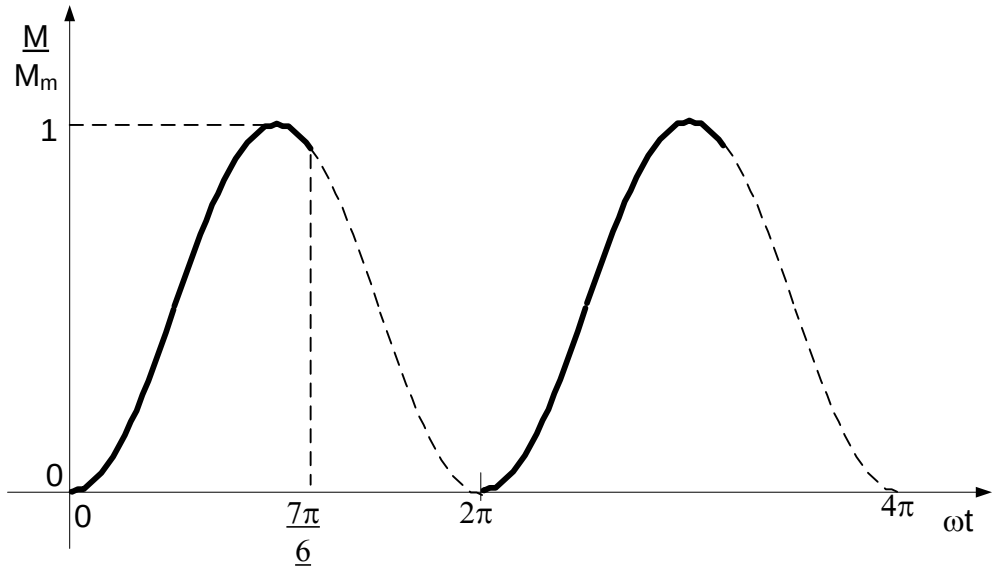

Fig. 4.3. Variation of torque M according to time t.

For a period π of i_b current, the torque M can be put in the form of:

$$\frac{M}{M_m}=\begin{cases}\frac{1}{2}(1-\cos\omega t); & \omega t\in\left[0;\quad\frac{7\pi}{6}\right]\\ 0; & \omega t\in\left[\frac{7\pi}{6};\quad 2\pi\right]\end{cases} \tag{4.3}$$

It should be emphasized that the friction element (fig. 4.1) weakens its adhesion to the disc at a decrease in elongation of 0.10...0.15 of its total value which corresponds approximately to the angle $\omega t = 7\pi/6$.

For the Fourier series development of the expression (4.3) relationships are used:

$$y(t)=M_0+\sum_{k=1}^{\infty}\left(A_{km}\sin k\omega t+B_{km}\cos k\omega t\right) \tag{4,4}$$

where:

$$M_0=\frac{1}{T}\int_{-\frac{T}{2}}^{\frac{T}{2}}M(t)\mathrm{d}t,\quad B_{km}=\frac{2}{T}\int_0^T M(t)\cos k\omega t\,\mathrm{d}t\quad A_{km}=\frac{2}{T}\int_0^T M(t)\sin k\omega t\,\mathrm{d}t, \tag{4.5}$$

The restricted form, in the sine, of the Fourier series (4.4), is:

$$M(t)=M_0+\sum_{k=1}^{\infty}M_{km}\cos\left(k\omega t+\alpha_k\right)\quad , \tag{4.6}$$

where:

$$M_{km}=\sqrt{A_{km}^2+B_{km}^2}\ ,\ \alpha_k=arctg\left(B_{km}/A_{km}\right) \tag{4.7}$$

For f = 100 Hz and $T = 1/f$ = 0.01 s, calculating the coefficients (4.5) – (4.7) with maple the maximum value of the M(t) function was considered conventionally equal to 1 because the results obtained can be easily adapted to the concrete situations.

For f = 100 Hz and $T = 1/f$ = 0.01 s, calculate the co-authors of the expression (4.4) with the Maple program. The maximum value of the function M(t) was conventionally considered equal to 1 because the results obtained can be easily adapted to the concrete situations.

M_0 average value M(t) function, the amplitudes of the harmonics as well as the phase shift between harmonics are shown in figures 4.4 and 4.5. .

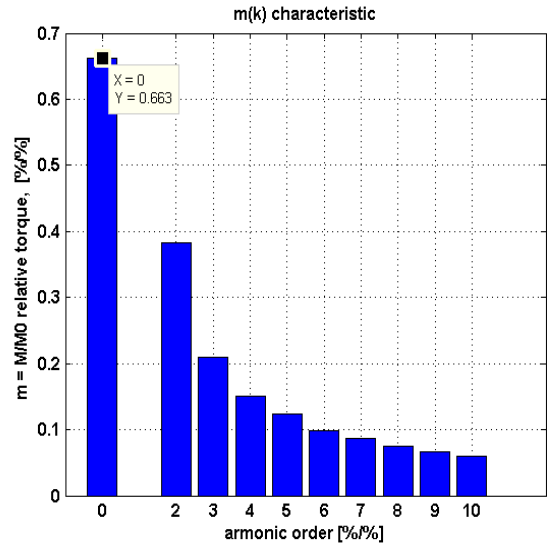

Fig.4.4. Mean value and harmonic amplitudes for the torque M.

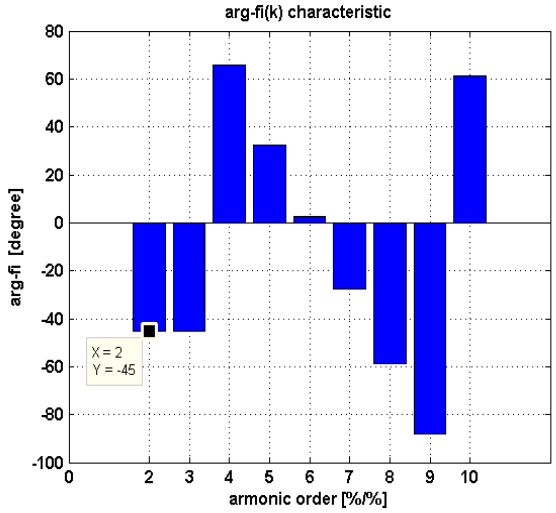

Fig. 4.5. The defams of the harmonics of the M couple.

From figure 4.4 it follows that the M_0 average value of the torqueis predominant, and harmonics of the order greater than three can be neglected. In the process of energy conversion in permanent regime, the average torque value is essential, the defams between harmonics (fig. 4.5) are of no interest in the process of energy conversion in these calculations. Harmonics can be of importance in the dynamic regimes of this engine. Collapse of the range $(0; 5\pi/6)$ leads to the reduction of the average torque value and therefore of the engine efficiency; this range must also be judged by experimental measurements.
It is found that the variation of torque M in figure 4.3 is periodic and has the period 2π. This form of variation of the torque M can be approximated with that shown in figure 4.6 and is used in the specialized literature only that the horizontal part of the curve is very small and is also adopted for experimental reasons.

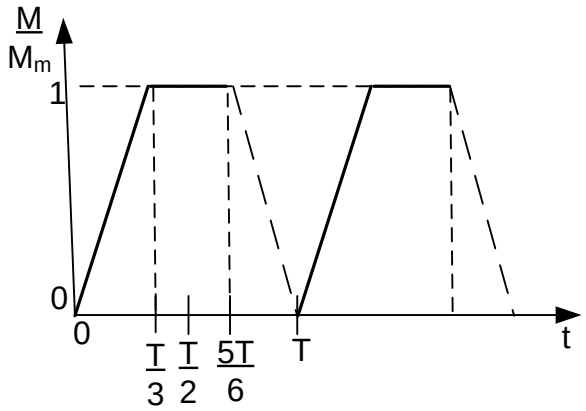

Fig. 4.6. Variation of torque M according to the time t.

For a period T, the torque M can be put in the form of:

M(t)= at; t € [0, T/3]

M(t)= 1; t € [T/3; 5T/6] (4.3)

M(t)= 0; t € [5T/6; T]

For fourier series development proceed as in the case of the function in figure 4.3.

The mean value of the M(t) function, the amplitudes of the harmonics as well as the phase shift between harmonics are shown in figures 4.4 and 4.5. .

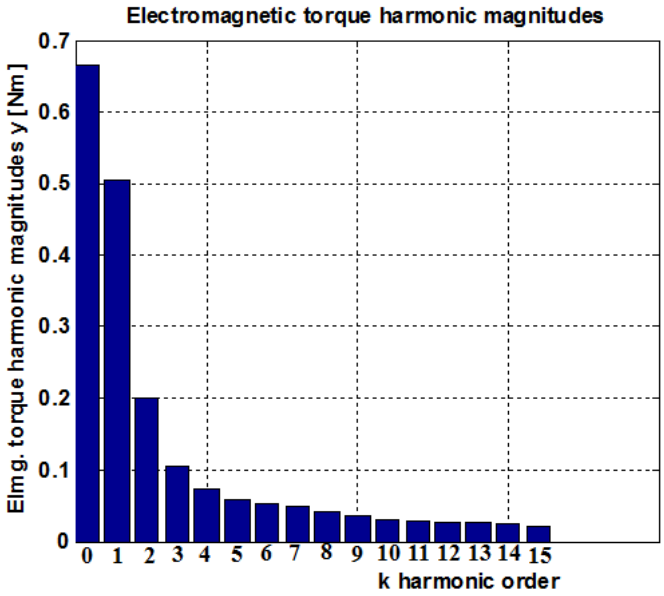

Fig. 4.7. Mean value and harmonic amplitudes for torque M.

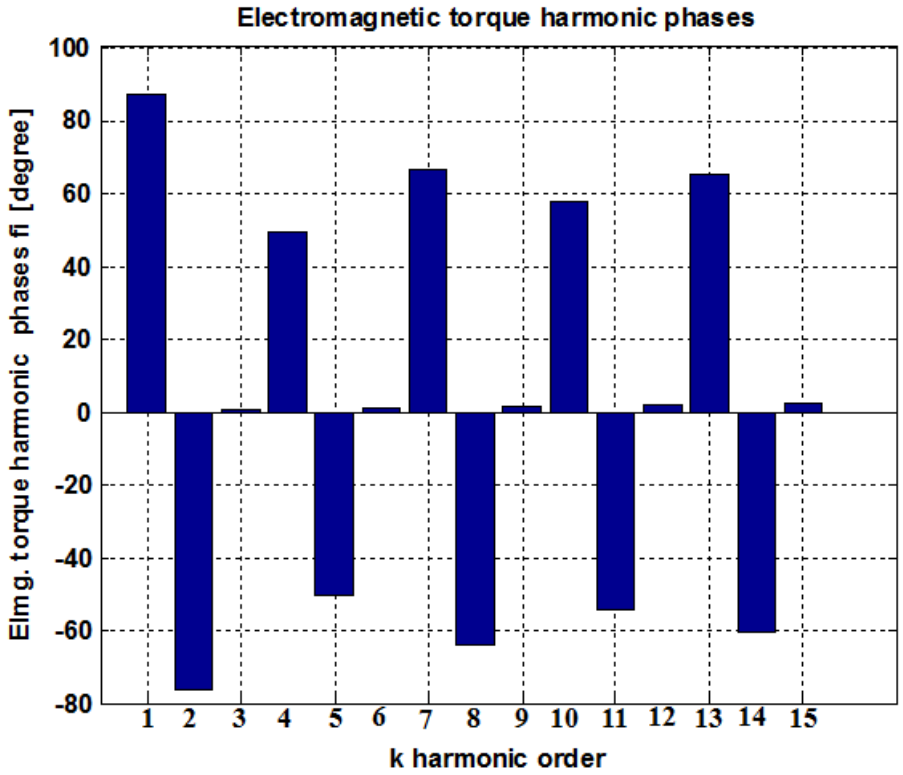

Fig. 4.8. The defams of the harmonics of the M couple.

From figure 4.7 it follows that the average torque value is predominant and has the value close to that in figure 4.4 and harmonics of the order greater than three can be neglected.

4.1. The torque transmitted to the rotor according to the current frequency.

It is considered a reference f_0 frequency and the mode of torque variation (fig. 4.6) for which the work is written in two variants: the work performed by the magnetostrictive bar (the first term in the relation (4.8)) is equal to the mechanical work performed by the mobile disk (the second term in the relation (4.8)), This equality is written for the frequency f_0 and for a certain frequency f, [54].

$$L_{m0} = \int_0^{\Delta L(T_0)} F_1(t)\, d(\Delta L) = \int_0^{\beta(T_0)} M_1(t)\, d\beta \quad {}_1$$

$$L_m = \int_0^{\Delta L(T_0)} F_f(f)\, d(\Delta L) = \int_0^{\beta(T_0)} M_1(f)\, d\beta \quad (4.8)$$

The notations are those in Figure 4.7. In this mathematical model, the expression of the revs is not directly deduced as a function of frequency, but one can deduce the torque M as a function of frequency, using the relations (4.8).
For frequencies f_0 (reference frequency) and f (a certain frequency) of the current ib in the coil, the torque at the two frequencies is represented in figures 4.9 a and b. One can write the

relationships:

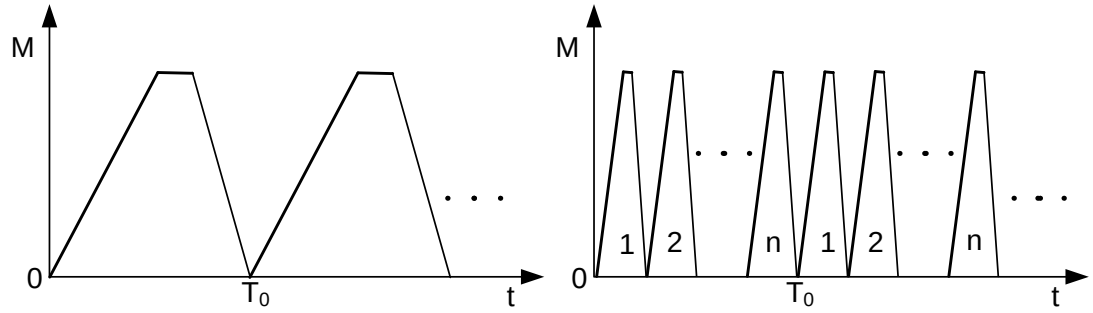

Fig.4.9 a) Torque M time-function at frequency f0 = 1 and T_0 period; b) Torque M function time at frequency f =nf0 and T = T0./n period.

$$\int_0^{\Delta L(T_0)} F_f(f)d(\Delta L) = \int_0^{\Delta L(T_1)} F_f(f)d(\Delta L) + \int_0^{\Delta L(T_2)} F_f(f)d(\Delta L) + ... + \int_0^{\Delta L(T_n)} F_f(f)d(\Delta L);$$

$$T_1 = T_2 = ...T_n = \frac{T_0}{n}$$

$$\Rightarrow \int_0^{\Delta L(T_1)} F_f(f)d(\Delta L) = \int_0^{\Delta L(T_2)} F_f(f)d(\Delta L) = ... = \int_0^{\Delta L(T_n)} F_f(f)d(\Delta L) = \int_0^{\Delta L(T_0/n)} F_f(f)d(\Delta L)$$

$$\int_0^{\beta(T_0)} M_f(f)d\beta = \int_0^{\beta(T_1)} M_f(f)d\beta + \int_0^{\beta(T_2)} M_f(f)d\beta + ... + \int_0^{\beta(T_n)} M_f(f)d\beta =$$

$$= n\int_0^{\beta(T_0/n)} M_f(f)\,d\beta = n\int_0^{\beta(T_0)} M_1(t)\,d\beta \Rightarrow \int_0^{\beta(T_0)} M_f(f)\,d\beta = n\int_0^{\beta(T_0)} M_1(t)\,d\beta \qquad (4.9)$$

The calculations in the relationship (4.9) were made over a period T_0 and are based on the properties of the definite integrals:

$$\int_a^{a+b} f(x)dx = \int_0^b f(x)dx = F(b) - F(0); \quad \int_a^b f(x)dx = \int_{a/k}^{b/k} f(kx)dx = F(b) - F(a) \qquad (4.10)$$

From the above relationships it follows that between the torqueM_f at the *f* frequency and M_1 torque at frequency f_9 = 1 Hz equality is achieved:

$$M_f = f\,M_1 \qquad (4.11)$$

From the relationship (4.11) it follows that the M_f torque developed at *f* frequency of the current supplying the coil is proportional to this *f* frequency.

This demonstration is valid for any type of variation over a period of the M_f size, but the same variation in time for any period.

The torque can also be modified by adjusting the amplitude of the current in the coil, but in a small area; torque is maximum when the amplitude of the current in the coil has the maximum allowable value.

4.2. Magnetomechanical conversion of energy to a rotary magnetostrictive motor.

In the process of magnetomechanical conversion of energy, the main element is the development of the mechanical work on account of the magnetic energy of the system for this

purpose, the mechanical work will be calculated according to the elongation of the material in the magnetostrictive process, [63, 64].
In the magnetic field the relationship between B magnetic induction, magnetic polarization $I = \mu_0 M = \mu_0 \varkappa_m H = k_m H$ (M este magnetizaţia magnetic polarization, $\varkappa_m$ is magnetic susceptiveness) and H magnetic field strength is in the form of:

$$\vec{B} = \mu_0 \vec{H} + \vec{I} = \mu_0 \vec{H} + \overrightarrow{\mu_0 M} \qquad (4.12)$$

The variation in the volume density of magnetic field energy for homogeneous bodies (vectors H and B are collinears) is:

$$d\,w_m = \vec{H}\,d\vec{B} = H\,d\left(\mu_0 H + I\right) = d\left(\mu_0 \frac{H^2}{2}\right) + H\,dI = d\,w_{mp} + d\,w_{mL}\,;$$
$$dw_{mp} = d\left(\mu_0 \frac{H^2}{2}\right);\quad dw_{mL} = H\,dI = d\left(k_m \frac{H^2}{2}\right) \qquad (4.13)$$

In the relationship (4.13) the size dw_{mp} is the own energy of the field in a vacuum and does not produce mechanical work; dw_{mL} is the energy that produces the mechanical work due to the presence in the magnetic field of the body with the magnetic polarization I and represents the mechanical work on the volume unit of the body with magnetic polarization. For the linear portion of the magnetostriction characteristic, the relationship can be written: $\Delta L = \lambda_M H$; the magnetic energy density can be calculated depending on the elongation of the ΔL that intervenes in the process of magnetomecanical energy conversion:

$$dw_{mL} = d\left(k_m \frac{H^2}{2}\right) = d\left(k_m \frac{(\Delta L)^2}{2\lambda_M^2}\right) \qquad (4.14)$$

According to the generalized forces theorems in the magnetic field (for constant current), one can calculate the developed force in the direction of elongation ΔL and then calculate the mechanical work L_{m1} developed by this force:

$$F_{\Delta L} = \frac{dw_{mL}}{d(\Delta L)} = k_m \frac{\Delta L}{\lambda_M^2} \quad \Rightarrow \quad L_{m1} = \int_0^{\Delta L}\left(k_m \frac{\Delta L}{\lambda_M^2}\right) d(\Delta L) = k_m \frac{(\Delta L)^2}{2\lambda_M^2} \qquad (4.15)$$

The last term in the relationship (4.15) shows that the work of the L_{m1} is proportional to the elongation of the ΔL to the square.
The mechanical work developed in the process of magnetostriction can be calculated in another way considering Hooke's law in the mechanics of elasticity.
The F force results from Hooke's relationship, $\Delta L = \lambda_H F$; elementary work is calculated dL_{m2}, where the work done L_{m2}, for a given ΔL elongation:

$$d\,L_{m2} = F\,d(\Delta L) = \frac{\Delta L}{\lambda_H} d(\Delta L) \Rightarrow L_{m2} = \frac{1}{\lambda_H}\int_0^{\Delta L} \Delta L\,d(\Delta L) = \frac{\Delta L^2}{\lambda_H} \qquad (4.16)$$

For adiabatic processes in which the elementary heat in the equations of thermodynamics δQ =0 it is obtained $L_{m1} = L_{m2}$.

$$L_{m1} = L_{m2} \Rightarrow \frac{k_m}{2\lambda_M^2} = \frac{1}{\lambda_H} \qquad (4.17)$$

In the relationship (4.17) the connection between the physical constants of material that have been previously presented is shown.
The relationships (4.15) and (4.16) established in this work highlight a remarkable fact; the mechanical work developed in the magnetostrictive process is proportional to the square of elongation ΔL, this means that only GMM (Giant Magnetostrictive Materials) materials must

be used for this engine. Currently, the preferred material is Terphenol-D although the mechanical properties are inferior to the Galphenol material, but the latter has an elongation of about 30% less, i.e. the mechanical work decreases by 50%.
It is considered the linear part of the magnetostriction caracracteristics (fig. 3.10.b); at the variation of the H field produced by the current ib that goes through the coil turns from the value – H_{bm} at H_{bm}, (fig.4.10.a), the increase of elongation ΔL occurs on the entire linear area so that a maximum elongation is obtained and this leads to high engine performance; TorqueM_1 , (fig.4.10.b) it has the maximum possible value for the magnetostrictive material used. If the magnetic field H_{mp} of the permanent magnet is closer to the magnetic field H_2 (fig.4.10.c) where the saturation zone begins, then the amplitude H_{mps} is noticeably smaller than the magnetic field H_2 and as a result, the magnetostrictive elongation is lower, and the performance of the actuator decreases even if *GMM* material was used. M_2 torque has a value less than the torque M_1 , (fig.4.10.d), $M_2 < M_1$.

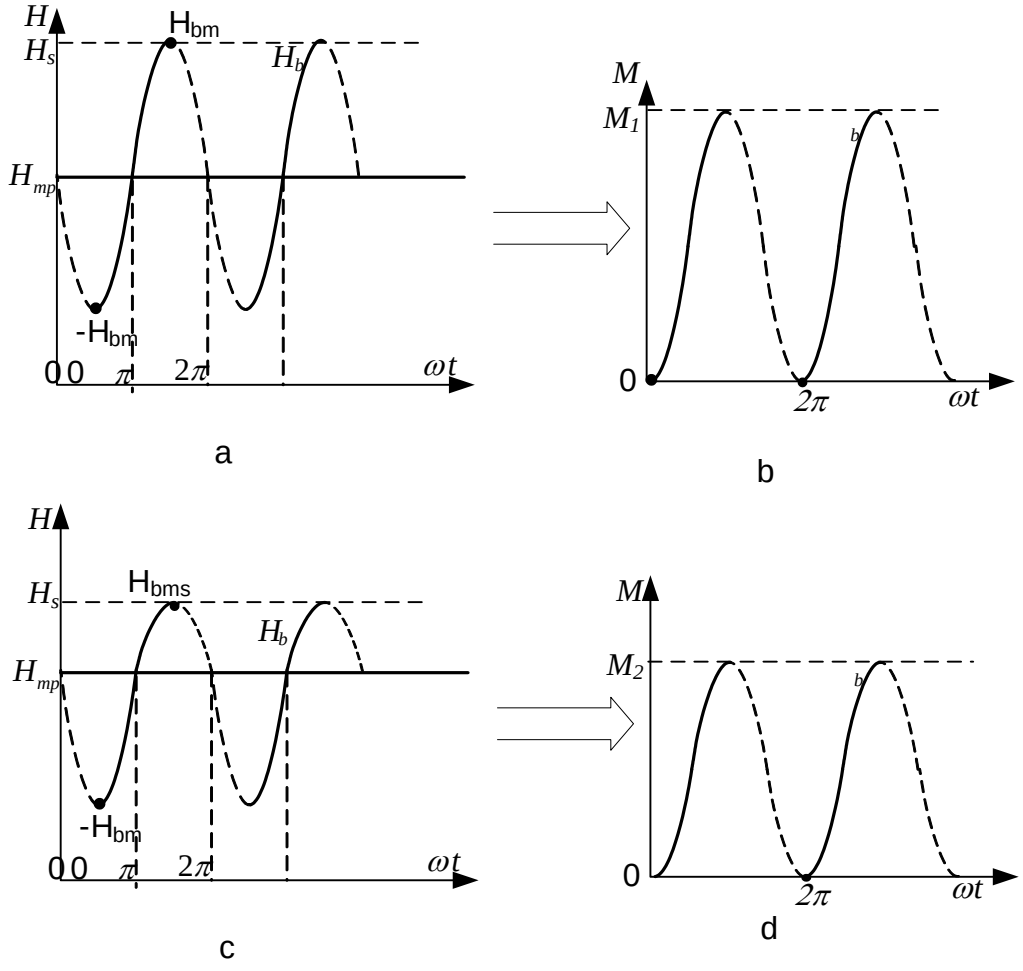

Fig. 4.10. The magnetic field H that produces the elongation of the magnetostrictive bar (the full line represents the active part of the torque acting on the rotor mobile disc) and the torque M developed by the magnetostrictive motor: a) H_{mp} magnetic field it is positioned in the middle of the linear portion of the elongation-field feature; b) Variation of torque M over time having the M_1 maximum value; c) H_{mp} magnetic field it is positioned near the saturated area. of the elongation - field feature; d) M torque variation in time having the M_2 maximum value.

For a high-performance actuator with GMM material equality is essential $H_{mp} = H_A$, (fig. 3.10.b).

4.3. Right return of the permanent magnet.

For the motor actuator it is necessary to analyze the displacement of the operating point of the permanent magnet on the right of return, the change in the position of the return right and the consequences regarding the performance of the actuator.
Considering that the magnetic flow of escapes of the permanent magnet can be neglected ($\Psi_{\sigma m} \equiv 0$) (fig. 4.4), then the equivalent magnetic scheme has the form of the figure 4.11. .

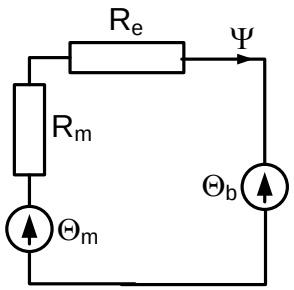

Fig. 4.11. The equivalent scheme of the magnetic circuit
with permanent magnet.

In this magnetic scheme were made notations: Θ_m = - HL_m is the equivalent solenation of the permanent magnet; Θ_b is the solenation of the coil considered demagnetizing; R_m – reluctance of the permanent magnet, R_e – reluctance of the outer circuit of the permanent magnet; Ψ – magnetic flux established in the magnetic circuit.
Based on the magnetic circuit in figure 4.11 and the notations in figure 4.4, the relationships can be written:

$$\Psi(R_m + R_e) = \Theta_m - \Theta_b \Leftrightarrow H L_m + S_m B(R_m + R_e) = -\Theta_b \; ; \quad \Psi = S_m B \; ; \quad \Theta_m = -H L_m \qquad (4.18)$$

From the relation (4.18) the equation between the H and B sizes of the permanent magnet is obtained:

$$H = -\frac{\Theta_b}{L_m} - \frac{S_m(R_m + R_e)}{L_m} B;$$

$$\Theta_b = 0 \Rightarrow \quad H = -\frac{S_m(R_m + R_e)}{L_m} B \qquad (4.19)$$

The second equation in the relationships (4.19) represents the equation of the right charge of the permanent magnet which, depending on the parameters of the magnetic circuit, positions the operating point on the demagnetization curve.
In paragraph 3.1 are presented a series of elements regarding the theory and equivalent schemes of the permanent magnets through which and the modification of the position of the return line, (fig. 3.3), which affect the H_{mp} magnetic field. P_1 is the point on the demagnetization curve that corresponds to the remaining magnetic induction; the right of return is parallel (approximately) with the tangent to the demagnetization curve at the P_1 point.

Consider the magnetisation state corresponding to the P_2 point , (fig. 3.3) , passing through the right return 1. The right load (denoted by 2 is translated by the size Θ_d/L_m to the left according to the first equation of (4.19); P_3 operating point for $\Theta_b = 0$ it moves in P_4 for $\Theta_d \neq 0$. It is possible that the Θ_b solenation of demagnetization to be of relatively high value and then the point of intersection of the right load with the demagnetization curve will be the point of intersection of the P' right load. In this case it changes and the right return and gets the right 3 passing through P'. For $\Theta_d \neq 0$, P_4 operating point it moves in P'_4. Magnetic induction in the P'_4 the point is less than the point P_4 namely $B'_4 < B_4$; this inequality is also maintained between the magnetic field intensities at these points (to a lesser extent) and results in a decrease in the H_{mp} field, that is, the value of the mechanical work developed by the system is affected.
The important result obtained in this paragraph is that the right of return remains the same always during operation; it is not allowed to appear in the coil current shocks with an amplitude greater than the maximum permissible amplitude established in the design.

4.4. The movement equation.

The expression of the n speed of any motor and in particular of the rotating magnetostrictive motor for any operating regime results from the equation of rotor movement; for the stationary regime when the angular speed of the Ω rotor it is constant, the equation becomes an algebraic relationship between couples (it is no longer a differential equation).
The equation of rotor motion has the form of:

$$J\frac{d\Omega}{dt} = J\frac{\pi}{30}\frac{dn}{dt} = M_a - M_r \ ; \quad M_r = M_D + M_L \rightleftarrows; \quad M_D = D\Omega \ ; \quad M_a = M_f \tag{4.20}$$

u where the M_r resistant torque (opposing the movement) has several components, the main component is the M_L load torque, other couples represent different types of mechanical friction or parasitic couples. In the relations (4.20) the notations were made: J – the moment of inertia of the moving part; M_D - viscous friction torque (friction in the bearings); M_L – load torque required by the operated installation (work machine). M_a – is the active torque
Mechanical characteristic, $n = f(M_L)$, of the magnetostrictive motor results from the equation of rotor motion (4.20) customized for the stationary regime in which the angular speed of the rotor Ω=ct., $\mathbf{M_L}$ = ct., $D \neq 0$ and results:

$$\Omega = ct. \ ; \quad \Rightarrow \ \Omega = \frac{\pi \ n}{30} = \frac{M_a - M_L}{D} \ \Rightarrow \ n = \frac{30}{\pi}\frac{M_a - M_L}{D};$$
$$M_a = M_f = f \ M_1 = F \ r_c \cos \ \alpha_0 = M \tag{4.21}$$

The data for the calculations are: $\cos\alpha_0 = 0{,}79$; $D = 23{,}6 \cdot 10^{-3}$ Nm/rpm
For $D = 0$ and $M_L = K\Omega^n$, results:

$$\Omega = ct. \ ; \quad \Rightarrow \ M_a - M_L = 0 \ \Rightarrow \ \Omega^n = \left(\frac{\pi \ n}{30}\right)^n = \rightleftarrows \ \frac{M_a}{K} \Rightarrow \ n = \frac{30}{\pi} \rightleftarrows \ \sqrt[n]{\frac{f \ M_1}{K}} \tag{4.22}$$

The two cases (4.21) and (4.22) show that the dependence of the n-rev on frequency has different forms depending on the dependence of the components of the M_r resistant torque of Ω angular speed, respectively depending on the speed n.

In the case of the magnetostrictive motor, the torque has the expression (4.6) and in this case the equation of motion has the shape.

$$J\frac{d\Omega}{dt} = J\frac{\pi}{30}\frac{dn}{dt} = M(t) - M_r = M_0 + \sum_{k=1}^{\infty} M_{km}\cos(k\omega t + \alpha_k) - M_r$$

$$M_r = 0 \quad \Rightarrow n = \frac{30}{J\pi}M_0 t + \frac{30}{J\pi}\sum_{k=1}^{\infty}\frac{M_{km}}{k\omega}\sin(k\omega t + \alpha_k) \qquad (4.23)$$

From the relations (4.23) it is found: :

1.The engine cannot run idle, the first term shows that the speed increases monotonously over time; this is explained by the fact that the M_0 torque value does not depend on the speed n and as a result the mechanical characteristic can not be defined for any M_L load torque, more the engine does not run stably (n=ct.) nor to the M_L constant torque load.

2.Percentage, the harmonics of the speed have amplitudes much lower than the harmonics of the couple, harmonics of the same order; the anplitudes of the harmonics of the rev are inversely proportional to the order of harmonics and the pulsation of the current in the coil; for subunit frequencies, the amplitudes of the harmonics of the rev can become important.

4.4.1. Establishing the variation in time of the Ω angular velocity based on a simplified mathematical model.

In the process of energy conversion at start-up and constant torque, the higher-order harmonics are neglected and taken into account only a part of the sinusoid of the first period of the torquefrom the first moments of the application of the tension and the presence of the M torque (fig. 4.12). Considering that at t = 0, the speed n = 0 is included and the starting range in which the operating point moves on the first segment of the magnetostrictive torque curve (fig. 4.3) after which in the following moments it continues with M_0 torque. In Figure 4.12 (full line) is represented this variation of torque which can be approximated with the following analytical relationship:

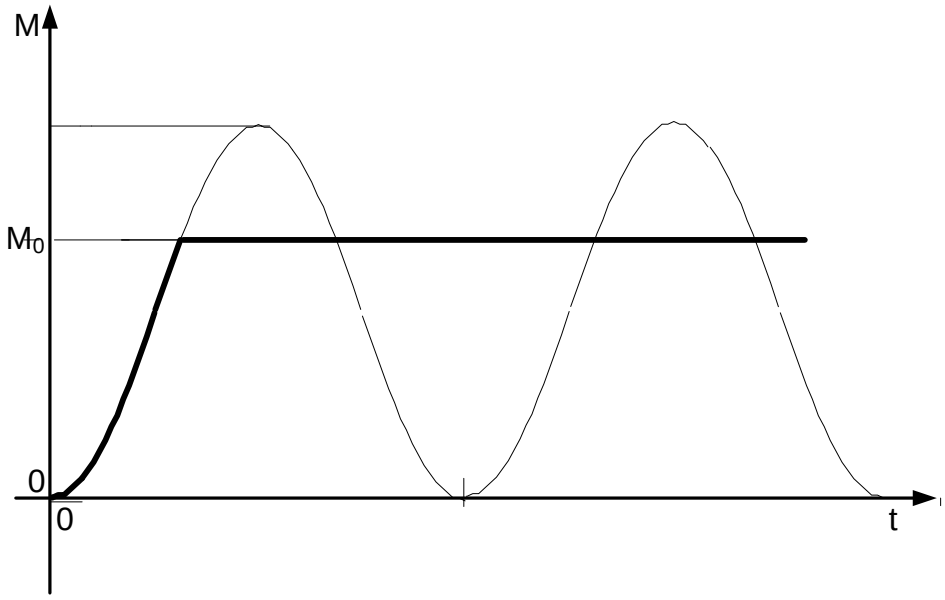

Fig.4.12. Variation in time (approximate) of torque M.

$$M = M_0\left(1-\exp\left(-\frac{t}{T_c}\right)\right) \qquad (4.24)$$

T_c time constant it is chosen as in the first moments the slope of the curve between 0 and M_0 (4.12) be approximately equal to that given by the relationship (4.24).
The equation of rotor motion, with the relation (4.24), determines the variation in time of the Ω angular velocity as it results from the following relationships:

$$J\frac{d\Omega}{dt} = J\frac{\pi}{30}\frac{dn}{dt} = M - M_r\ ; \quad M_r = M_C + M_D + M_L \rightleftarrows; \quad M_D = D\Omega\ ; \quad M_C = ct.$$

$$J\frac{d\Omega}{dt} = M - M_r = M - (M_C + M_D + M_L); \quad M = M_0\left(1 - exp\left(-\frac{t}{T_c}\right)\right)$$

$$\Rightarrow \quad \frac{d\Omega}{dt} + \frac{D}{J}\Omega = \frac{M_0}{J}\left(1 - exp\left(-\frac{t}{T_c}\right)\right) - \frac{M_C + M_L}{J} = k_{m1} - k_{m2}\,exp\left(-\frac{t}{T_c}\right).$$

$$\frac{d\Omega}{dt} + k\Omega = k_{m1} - k_{m2}\,exp\left(-\frac{t}{T_c}\right)\ ; \quad k = \frac{D}{J}\ ; \quad k_{m1} = \frac{M_0 - (M_C + M_L)}{J}\ ; \quad k_{m2} = \frac{M_0}{J}$$

$$\Rightarrow\ \Omega = \frac{k_{m1}}{k} - \frac{k_{m2}}{k-1/T_c}exp\left(-kt - \frac{t}{T_c}\right) + \left(\frac{k_{m2}}{k-1/T_c} - \frac{k_{m1}}{k}\right)exp(-kt) \quad ; \quad T_c < \frac{T}{3} \quad (4.25)$$

M_C is the coulomb type friction torque considered constant (M_C = ct.).
For the k = 0 factor and M_r=0 (that is, ideal idling), equation of movement and Ω angular speed have the expressions:

$$J\frac{d\Omega}{dt} = M = M_0\left(1-\exp\left(-\frac{t}{T_c}\right)\right) \Rightarrow \quad \Omega = \frac{\pi n}{30} = \frac{M_0}{J}t + \frac{M_0}{J}T\left[\exp\left(-\frac{t}{T_c}\right)-1\right] \quad (4.26)$$

From the relations (4.26) it is found that without the factor k, which represents the motor load, the magnetostrictive motor cannot operate stably. If the factor k is different from zero, then the Ω angular velocity stabilizes at a constant value after the first moments of the start-up process.
For high values of the time t, the permanent regime is reached; the expression of the angular velocity in (4.25) becomes:

$$t \to \infty\ \Rightarrow\ exp\left(-kt - \frac{t}{T_c}\right) \equiv 0\ ; \quad exp(-kt)\ \equiv 0\ \Rightarrow\ \Omega = \frac{\pi n}{30} = \frac{k_{m1}}{k} = \frac{M_0 - (M_C + M_L)}{J}$$

$$k \to 0\ \Rightarrow\ \Omega \to \infty$$

(4.27)

Expression of Ω angular velocity (4.27) represents the mechanical characteristic of the rotary magnetostrictive motor Ω = f(M_L) or n = f(M_L) , which is a right fall with the increase of the torque of load M_L; at k = 0 , the engine increases its speed.
This mathematical model for the study of the engine is of interest in the short-term regimen; such as in rotating a part with a certain angle as is the case in robotics, but it can also be adapted to the intermittent operating mode of the engine.

5. Construction of the rotary magnetostrictive motor.

Within the Department of Micro and Nanoelectrotechnologies of ICPE-Romania, a rotating magnetostrictive motor was made in which the actuation is made on the plane of the rotor disc; figure 5.1 shows the main constructive components:
1 – magnetostrictive actuator;
2 – positioning system of the magnetostrictive actuator;
3 – rotor disk

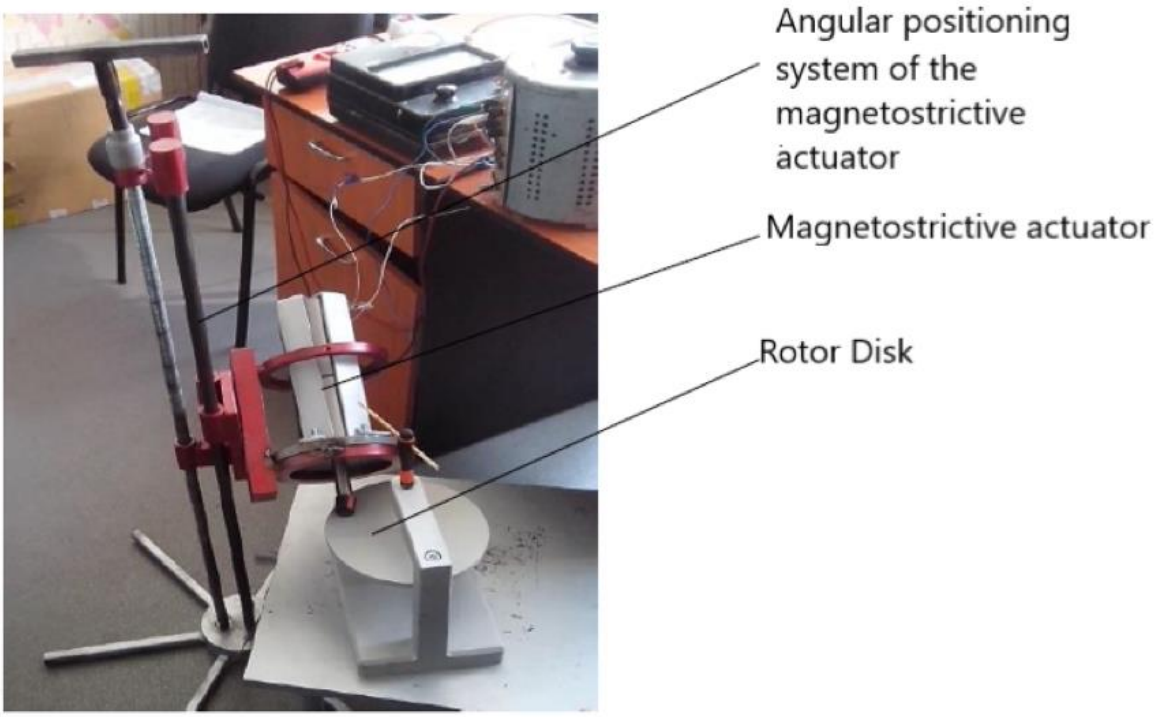

Fig. 5.1 Rotary magnetostrictive motor, main components.

Components 2 and 3 were made; the pieces of these components were made at ICPE – Romania, and others at the Institute of Fine Mechanics.
In Figure 5.2. the structure of a magnetostrictive actuator (actuator operating on the rotor disc) is presented, and in figure 5.3. the main landmarks of this actuator are presented.

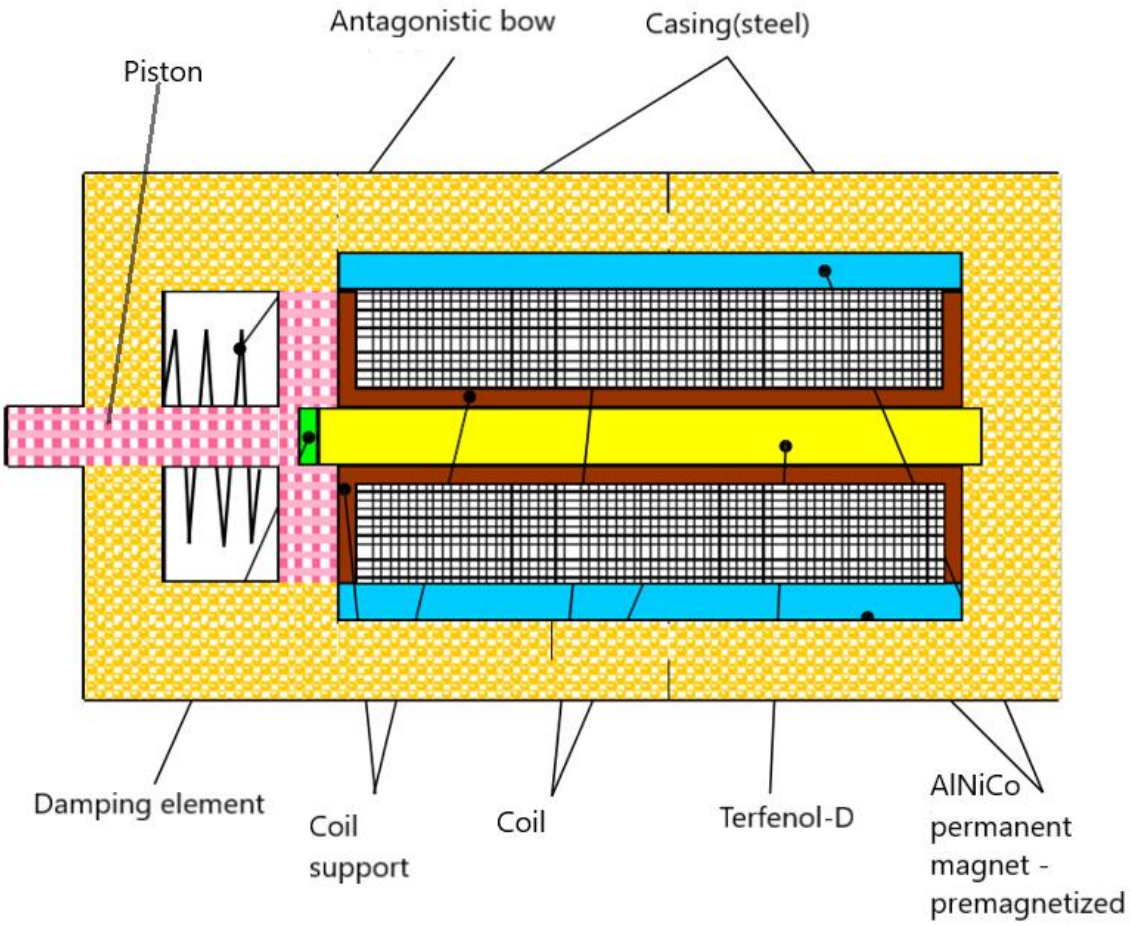

Fig.5.2. The structure of a magnetostrictive actuator.

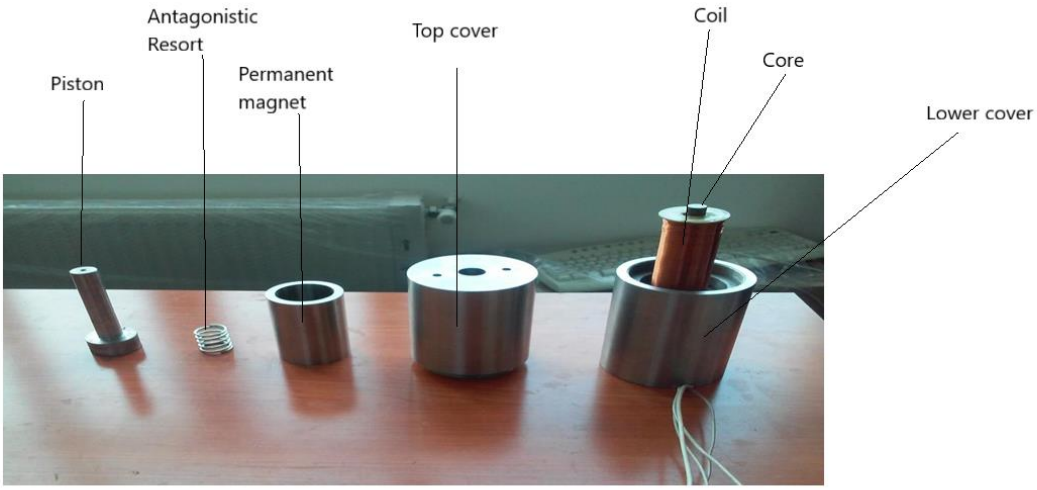

Fig.5.3. The main highlights of the actuator.

5.1. Positioning system of the magnetostrictive actuator.

This system (fig. 5.4) has the role of positioning the actuator in relation to the rotor disc and obtaining the optimum α0 inclination angle of the e-body element of friction to the rotor surface, figure 4.1. .

Fig. 5.4. Positioning system of the magnetostrictive actuator, general view.

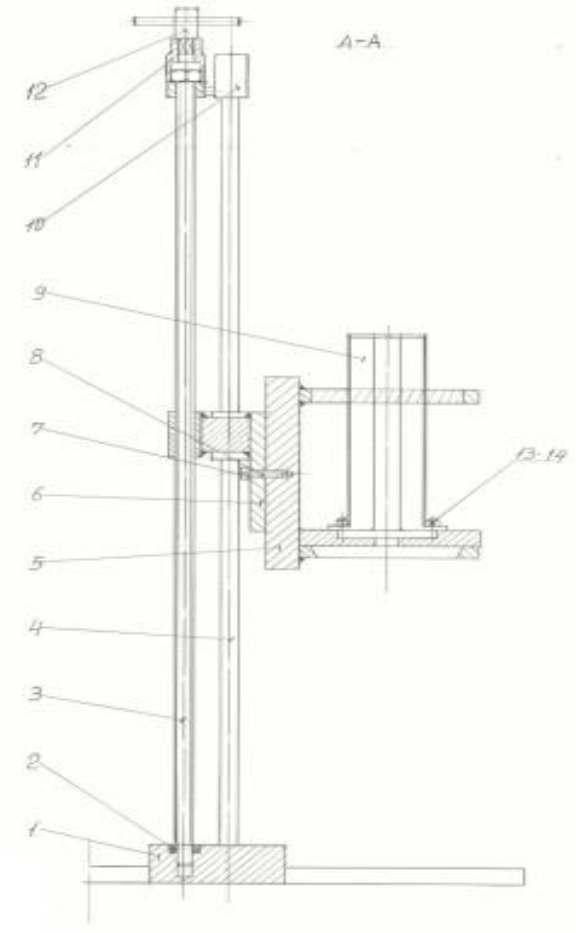

Fig. 5.6. Vertical section of the positioning system.

Table 5.1 shows the pieces of the positioning system by numbering in figures 5.5 and 5.6. .

Table 5.1. Parts of the positioning system

Position	Name	Drawing number(STAS)	Pieces	Material	Obs.
1	Plateau		1	OLC45	Assembly
2	Axial bearing	Seria 51102	1	RUL.	Commerce
3	Threaded column		1	Group 6-8	Assembly
4	Column		2	OLC45-tras	
5	Tiltable support		1		Assembly
6	Mobile support		1		Assembly
7	Spring plate		1		Commerce
8	M8x35 Screw	STAS	1	Group 8-10	Commerce
9	Lamella lock		4	OL-50	
10	Guide support		1		Assembly
11	S27 Key		1	Crom-Vanadiu	Commerce
12	Trainer		1	OLC45	
13	M8x25 Screw	STAS 5144	8	Group 8-10	Commerce
14	M8 Nut	STAS	8	Group 6-8	Commerce

Technological elements and drawings with dimensions of the component parts are shown in Annex 3.

5.2. Mobile system (Disc rotor).

Figure 5.7 shows the overview of the mobile system. The disc rotor is composed of three constructive elements: disc, spindle and bearings; In figure 5.8 are presented the three projections in the three-dimensional system in which the structure of this subassembly of the magnetostrictive motor is highlighted, and in table 5.2 the characteristics of the component parts are presented.

Fig. 5.7. Overview of the mobile system.

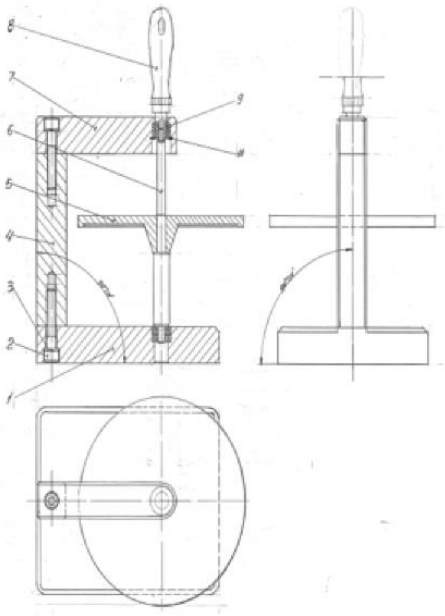

Fig. 5.8. Technical drawing of the disc rotor.

6. Measurements in the experimental study.

The measurement system has been developed and adapted to the requirements of the new engine. A test stand specific to magnetostrictive motor tests includes: transformer, voltage amplifiers, static frequency converter and measuring devices (digital voltmeter, digital ammeter, oscilloscope, micropalpator, dynamometers for measuring forces - Swiss Correx type with measure range 0.2 – 200 cN, torcmeter for measuring couples - in English torquemeter).
A test stand specific to the tests of the magnetostrictive motor is shown in fig.6.1.

a

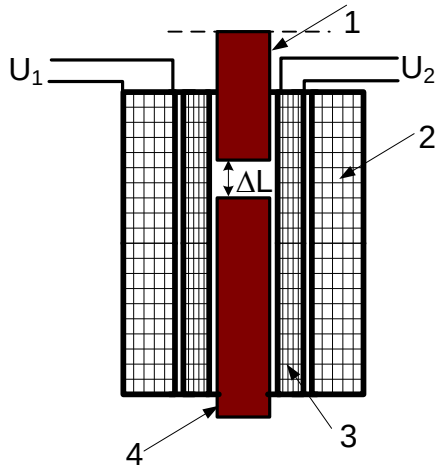

b

Fig. 6.1. Sample stand for a rotary magnetostrictive motor (see Fig. 5.1.): a) torchmeter (torquemeter); (b) the basic outline of the operation of the micropalpator:
Like other types of appliances, the torcmeter is a device that through a device called a torque transducer converts torque into an electrical signal, which can be processed by measuring instruments or computers.

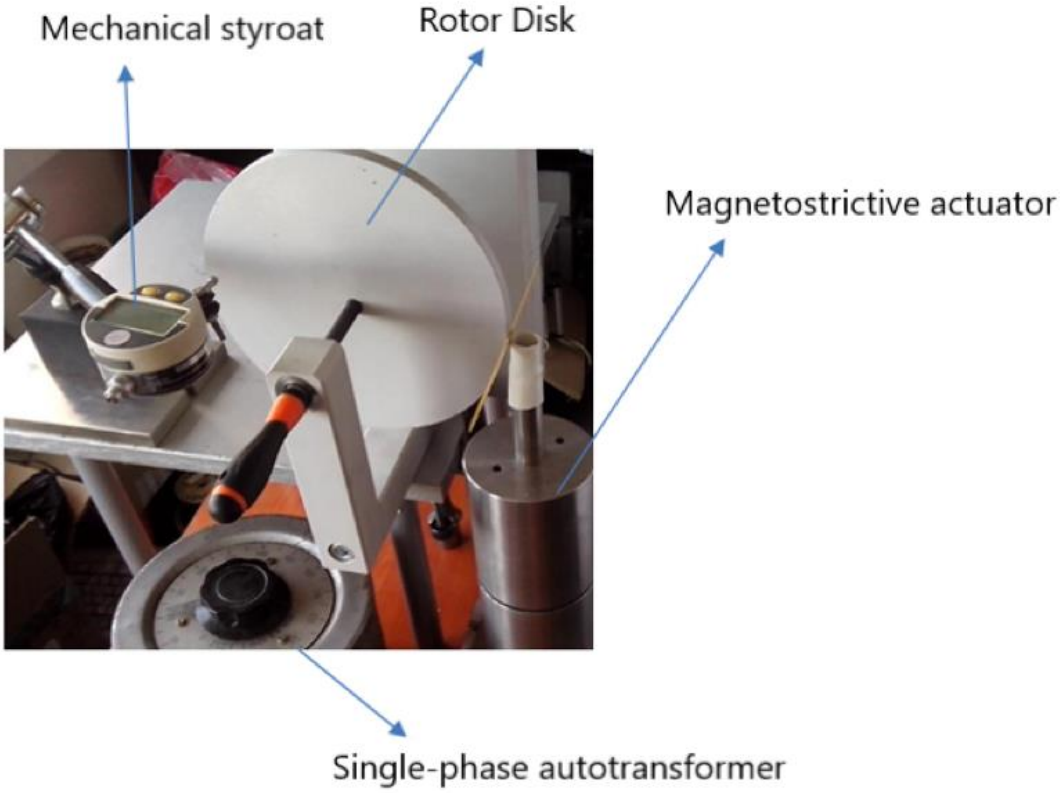

Fig.6.2. The way of fixing the styroater for measuring the beats and deviation of the disc rotor surface in axial direction and the sample stand for the magnetostrictive motor

The construction of the micropalpator is, in principle, similar to the transformer with the difference that there is an air space ΔL having the height equal to the maximum value of the magnetostrictive elongation, (fig. 6.1.c). When feeding the coil of the actuator (the primary) with a frequency current f, then the betweenfier changes with the frequency 2f; with the same

frequency, the reluctance of the interfier area is also modified. If the primary winding of the micropalpator is fed with the U_1 voltage, then through the magnetic circuit (consisting of rods and the outside of the coils) a flow is established that will vary in time with the frequency 2f and will induce in the secondary winding an electromotor voltage, at the terminals, this is how the U_2 voltage is obtained which is then transmitted to a special apparatus to which the magnetostrictive elongation can be read directly. The stypator was also used to check the flatness of the disc rotor (fig. 6.2).

7. Experimental data and simulations.
7.1. Experimental data.

For the PhD thesis, within the Department of Micro and Nanoelectrotechnologies from ICPE-Romania, a rotating magnetostrictive motor was made in which the actuation is made on the plane of the rotor disc. The engine was made in order to verify the theory elements elaborated in this paper: the A_T point position determined by the magnetic field of the permanent magnet (fig.5.b), measurement of elongation and magnetostrictive force depending on the magnetic field, Hooke's constant; experimental mechanical characteristic. An experimental method was elaborated to verify the position of the A_T point which was applied to the actuator of the made engine. For performing experiments, the engine is provided with an angular positioning system of the actuator that allows performing a large number of experiments; the experimental study was part of several published articles,[61].

A. A first set of experiences refers to the variation of torque developed by the motor depending on the frequency of current that travels through the coil. The M_r torque value was taken as a reference measured at 50 Hz, then calulate the other values. The data in Table 7.1 show the proportionality between the torque acting on the rotor disc and the frequency of the current supplying the actuator coil, i.e. the relationship (4.11); the deviations are found to be technically acceptable. These measurements were made for different values of the actual current in the coil from which the data in Table 7.1 were retained, all the experiments performed confirm the relationship (4.11).

Tabelul 7.1

I =2 A

f [Hz]	M_f [Nm] Calculated	M_f [Nm] Measured
50	$11 \cdot 10^{-3}$	$11 \cdot 10^{-3}$
80	$17{,}6 \cdot 10^{-3}$	$15.5 \cdot 10^{-3}$
100	$22 \cdot 10^{-3}$	$21{,}3 \cdot 10^{-3}$
120	$26{,}4 \cdot 10^{-3}$	$26 \cdot 10^{-3}$
150	$33 \cdot 10^{-3}$	$31 \cdot 10^{-3}$

B. The next experimental test consists in checking the coincidence of the operating point of the permanent magnet with the point in the middle of the linear portion of the magnetostrictive characteristic. In the work was elaborated a method with two variants for this verification, (fig. 3.10). This verification can be done both by recording the variation in time of the ΔL elongation, as well as by supplying the coil in direct current with changing the direction of the current. The experiments carried out in this case took into account the direct current supply of the actuator's coil. In table 7.2 data are given on the two directions of the direct current.

Important is the measurement at a maximum allowable current for the coil in order to take into account the entire linear area of the magnetostrictive material used.

Tabelul 7.2.

I [A]	1,1	1,8	2,25	3
ΔL [μm = 10^{-6}m]	12	18	21	25
-I [A]	-1,1	-1,7	-2,18	-3
ΔL [μm = 10^{-6}m]	9,8	17,1	20,4	23,8

Experimental data from Table 7.2 show that the positions of the two magnetic fields H_{Am} and H_A correspond to the performance performance ,(fig. 3.10.d). Differences between size ΔL values, *at the same current value, for the two directions are acceptable. The method can be used for any type of actuator, especially for prototypes, to determine the concordance between experimental data and design data. It can also be used for checks after certain periods of operation of the actuator.*

C. Mechanical characteristic of the magnetostrictive motor, $n = f(M_L)$, results from the rotor movement equation customized for the stationary regime, in which the angular speed of the rotor Ω is constant for constant load couple; the torque M is calculated with the relation (4.2.). The relation (4.21) represents the equation of mechanical characteristic in which the rotational speed n depends linearly on the M_L torque. The measurements are presented in Table 7.4. .

Tabelul 7.4.

U[V] Measured	f [Hz] Measured	n[rpm], Measured	n[rpm] Calculated	M[Nm] Calculated	M_L[Nm] Measured
100	*100*	12	12,3	$30{,}4\cdot10^{-3}$	0
100	100	6	6,22	$30{,}4\cdot10^{-3}$	$15\cdot10^{-3}$
100	100	5	5,01	$30{,}4\cdot 10^{-3}$	$18\cdot10^{-3}$
100	100	3,5	3,39	$30{,}4\cdot 10^{-3}$	$22\cdot10^{-3}$
100	100	1,5	1,78	$30{,}4\cdot 10^{-3}$	$26\cdot10^{-3}$
100	150	15	16,08	$39{,}8\cdot 10^{-3}$	0
100	150	8	7,6	$39{,}8\cdot 10^{-3}$	$21\cdot10^{-3}$
100	150	7	6,72	$39{,}8\cdot 10^{-3}$	$23\cdot10^{-3}$
100	150	5	4,76	$39{,}8\cdot10^{-3}$	$28\cdot10^{-3}$
100	150	3	2,75	$39{,}8\cdot 10^{-3}$	$33\cdot10^{-3}$

It is found that idling speed is limited by losses in camps according to the equation of movement (4.20), M_D torque; for D = 0 it theoretical results $n \rightarrow \infty$.
Table 7.4 shows the values for two mechanical characteristics, $n = f(M_L)$, for U =100 V, f = 100 Hz and for U =100 V, f = 150 Hz. It has been observed that the differences between the measured and calculated speeds are below 10%, which can be considered acceptable. The D constant was determined by several tests on the engine using the relationship (4.21).
The experimental tests carried out shall involve, inter alia:
- method of experimental verification of the operating point of the permanent magnet and the coincidence of this point with the middle of the linear portion of the elongation-field characteristic;
- determination of the active torque at the motor axis by measuring the developed force at magnetostriction and multiplying it by the radius of the point of contact of the elastic element of friction with the rotor disc;

- the mechanical characteristic of the motor at constant load torque (does not depend on the rotation speed) and for high torque values has been established M_L that tends towards a straight line with a negative slope in the reference system (M_L, n), $M_L \neq 0$.

7.2. Simulations of the movement equation.

Based on the information shown in paragraph 4.4 (equation of motion) the equation of movement shall be presented in the form of:

$$\frac{dn}{dt} = \frac{30}{J\,\pi} M_a - \frac{30}{J\,\pi}\left(M_0 + D\,\Omega + K\Omega^n\right); \quad n > 1 \qquad (7.1)$$

The M_a torque has the form shown in figure 4.3. .
The simulations performed are shown in figure 7.2. .

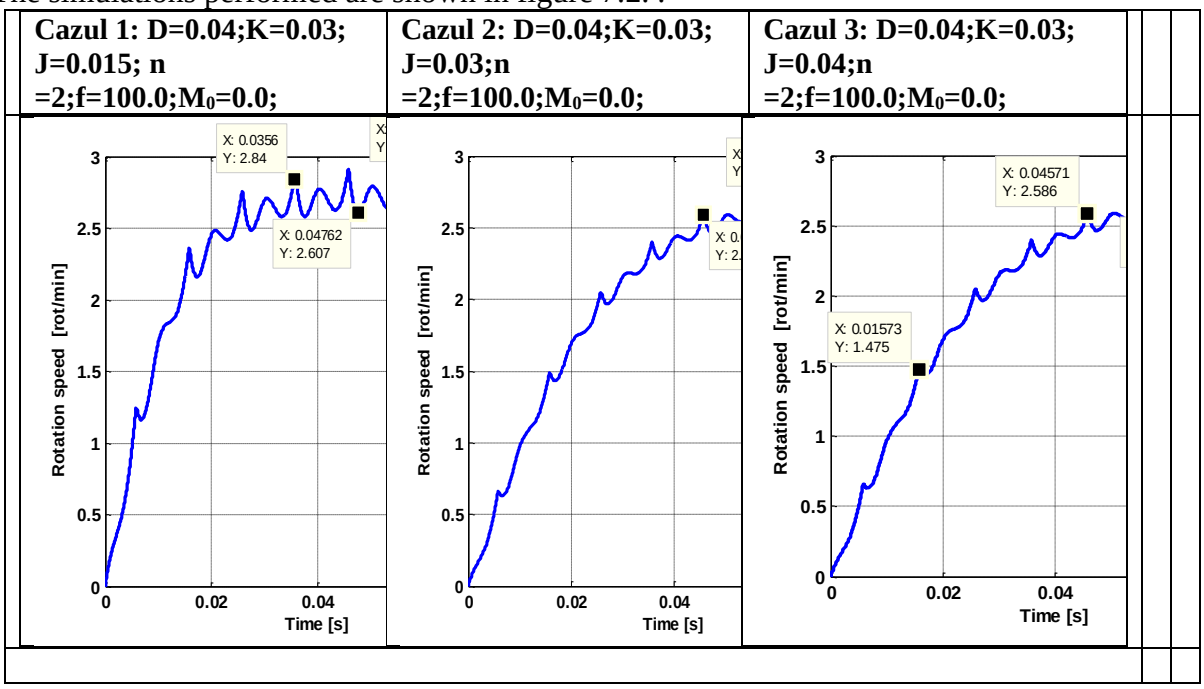

Fig. 7.1. Motion equation simulations 7.1 for n= 2

In equation 7.1 the torque of losses in the bearings is present $D\,\Omega$ and the $M_L = M_L + K\Omega^n$ load torque; in the technique of electric drives M_L load couples are of a very large variety, in this work was chosen a commonly used form.
M_a torque it has a periodic variation in time, which determines the starting process, the oscillations that occur in the curve of the sund speed determined by this torque; the amplitudes of these oscillations decrease with the increase of the J. moment of inertia The start time having a short duration does not significantly change the shape of the curve.

8. Original contributions and published works through which the obtained results were disseminated.

The results obtained in this work allow an improvement of the design system and an efficient use of magnetostrictive materials for the engine to operate at high performance. The following is a brief presentation of the main contributions made in this phd thesis.

● For a precise interpretation and calculation of the reluctance of the sections of the magnetic circuit, which have losses through hysteresis, the hysteresis cycle was analyzed, it was equated with two components: a component that corresponds to the reversible magnetization processes represented by a line and a component that corresponds to the irreversible magnetization processes represented by an ellipse whose axes coincide with the coordinate axes. The components (μ_r'si $\mu_r^{"}$.) of complex permeablity are interpreted geometrically and lead to the calculation of the two reluctances: R_c – conservative reluctance (the real part of complex reluctance) and R_d – dissipative reluctance (the imaginary part of the complex reluctance) and not the inductive reaction as it is used in some works; The reluctantes of the magnetic circuit must be calculated precisely and over certain frequencies the dissipative reluctantes for the ferromagnetic sections of the magnetic circuit should not be neglected.

● It is emphasized the sequence of phenomena that lead to the appearance of magnetostriction: uncompensated magnetic spin moments of the atom of the magnetostrictive material; depending on the available energy, they are ordered on energy shells and the atom has a resulting magnetic moment different from zero; Weis domains of parallelepipedic shape are formed and each domain contains a large high of atoms, the magnetic moments being parallel and the result is the spontaneous magnetization different in value of zero; in an external magnetic field, these domains are oriented in the direction of the field and the phenomenon of magnetostriction is obtained.

● In the process of magnetomechanical energy conversion, as well as the transmission of energy between physical systems, the mechanical work has an essential role, obviously, this is also true in the process of magnetomecanical energy conversion, (for adiabatic systems if $\delta Q = 0$). The work transmitted to the rotor disc depends essentially on the elongation of the material under the influence of the magnetic field H; only for large size of ΔL values, an advantageous electromechanical conversion takes place, it is established that the work is proportional to the value of the ΔL elongation squared.

● It is proved that the efficient operation of the actuator takes place when the operating point of the permanent magnet coincides with the value of the magnetic field at the half of the linear portion of the elongation-field characteristic of the magnetostrictive material used (the area where the slope is maximum), a high torque is obtained and the coil has a low consumption of electricity.

● It was elaborated an experimental method of checking the situation from the previous point in two variants: a) the recording of the variation in time of the elongation and the interpretation of its form; b) the dc power supply of the coil and the elongation is measured for the direct direction and then for the reverse direction of the current. If the two elongation values are equal, then the required data correspond. This method is of interest for prototypes; in order to obtain the desired solution, the reluctance of some areas of the magnetic circuit is modified. The method may also be used for regular checks during engine operation.

. ● Using the equality between the mechanical work developed by the magnetostrictive bar and the torque that sets in motion the rotor disc, it is proved that the M_f torque value developed at f frequency of the current supplying the coil is proportional to this f. frequency, namely:

$$M_f = f M_1$$

Where M1 is the torque value at frequency $f_0 = 1$ Hz .

This demonstration is valid for any type of variation over a period of the M_f, size but have the same variation in time for any period, otherwise the established relationship becomes a sum in which the number of terms is equal to the frequency of the current.
The torque can also be modified by adjusting the amplitude of the current in the coil, but in a small area; torque is maximum when the amplitude of the current in the coil has the maximum allowable value.

● From the equation of rotational motion we obtain the variation of the speed depending on the shape of the M_r resistant torque; if this torque is constant, then a permanent regime is not obtained – in particular – the engine cannot run idle. For a permanent operation it is necessary and sufficient as only a component of the M_r resistant torque; depend on the speed. The shape of the mechanical characteristic depends on the mode of variation depending on the speed of the M_r torque components. They can operate in high-performance conditions in short-term mode (close to the intermittent regimen) as it happens in robotics, medical technique.

● The author has developed within the Department of Micro and Nanoelectrotechnologies in ICPE-Romania a rotating magnetostrictive motor, has dimensioned and executed the fastening system and the mobile system, part of the parts were made at the Institute of Fine Mechanics.

● The measurement system has been developed and adapted to the requirements of the new engine. Two class D voltage amplifiers were used for this application which represents a new way of achieving the doubling of the amplitude of the output signal between 50-150 Hz. An assembly was used, which also includes a transformer, a voltage driver connected to a signal generator, an oscilloscope and the magnetostrictive actuator.
The assembly consisting of generator, amplifier, transformer, oscilloscope, multimeter forms the minimum platform for the measurements made at the magnetostrictive actuator. The assembly necessary to obtain the desired amplitude and to display its size in order to study the elongation and contraction of the ferromagnetic core regulating in real time the supply voltage of the actuator.

● There have been elaborated articles in connection with the subject of the thesis that were published at conferences and symposiums: below are presented these works:

[1’]**. Alexandru Dalea**, Mircea Ignat, Sorin Deleanu, Mihai Iordache, Neculai Galan, **“The Rotary Magnetostrictive Motor: a Promising Solution for Low Power Actuators”**, Annals of the University of Craiova, Electrical Engineering series, No. 42, Issue 2, 2018; ISSN 1842-4805, pp. 10 - 28.
[2’]**. Alexandru Dalea**, Mircea Ignat, Sorin Deleanu, Mihai Iordache, Neculai Galan, **„Consideraţii privind funcţionarea motorului magnetostrictiv rotativ”**, Proc. SME’16 Ediția a XII-a, București 9 noiembrie 2018 ISSN: 1843-5912, pe CD, pp. 61-72.
[3’]**. Alexandru Dalea,** Mircea Ignat, Sorin Deleanu, Mihai Iordache, Neculai Galan, **“Optimal Operation of the Rotary Magnetostrictive Motor“**, Publisher: IEEE, IEEE Xplore, 2018 International Conference on Applied and Theoretical Electricity (ICATE),
DOI: 10.1109/ICATE.2016.7754705, 978-1-5386-3806-4/18/$31.00 ©2018 IEEE, Page(s): 1 – 6.
[4’]**. Alexandru Dalea**, Mircea Ignat, Mihai Iordache, Neculai Galan, **„Rotary Magnetostrictive Motor”**, Proc. of the 12th International Conference on Electromechanical and Power Systems, SIELEM 2019, October 11-14, 2019, Chişinău Rep. MOLDOVA, IEEE Xplore, 978-1-4673-7488-0/15/$31.0 2015IEEE, **DOI:** 10.1109/SIELMEN.2017.8123295 , **Publisher:** IEEE, pp. 1-7 (in press).
[5’]. Mircea Ignat, **Alexandru Dalea**, **“Short Introduction on the Magnetostrictive Motor”,** National Institute for Research and Development in Electrical Engineering (INCDIE ICPE-CA), Splaiul Unirii, No. 313, District 3, 030138, Bucharest, Romania, ISSN: 2069-1505.
[6’]. **DALEA A.**, IGNAT M., DELEANU S., IORDACHE M., GALAN N., **“New Aspects in Rotary Magnetostrictive Motor Operation”**, in Electrotehnica, Electronica, Automatica (EEA), 2018, vol. 66, no. X, pp. XX-XX, ISSN 1582-5175.

● Articles have been elaborated in connection with the subject of the thesis that have only been communicated:

[7’]. Mircea Ignat, **Alexandru Dalea**, Neculai Galan, *INCDIE ICE CA,**UPB-Facultatea de Inginerie Electrica, “**Incercarile preliminare ale unui motor magnetostrictiv”**, SIMPOZIONUL DE MAŞINI ELECTRICE SME’15– 23 Octombrie, 2015.
[8’]. Mircea Ignat, **Alexandru Dalea**, Neculai Galan,**” Motor magnetostrictiv rotativ”**, SIMPOZIONUL DE MAŞINI ELECTRICE SME’15–23 Octombrie, 2015.
[9’]. Mircea Ignat, **Alexandru Dalea**, Neculai Galan,INCDIE ICE CA,**UPB-Facultatea de Inginerie Electrica, **“ASPECTE TEORETICE SI EXPERIMENTALE PRIVIND REGIMUL DINAMIC AL CONTACTULUI MECANIC LA MOTORUL MAGNETOSTRICTIV ROTATIV”**, SIMPOZIONUL DE MAŞINI ELECTRICE SME’16 – 11 Noiembrie, 2016.
[10’]. **Alexandru Dalea**, Codarnai Mihai, Ion Ion-Aurel, **“MOD DE ALIMENTARE A ACTUATORULUI MOTORULUI MAGNETOSTRICTIV”**, SME’17-10 noiembrie, Editia 13, UPB Bucuresti.

BIBLIOGRAPHY

[1]. *E. Burzo*, "Fizica fenomenelor magnetice(Physics of the magnetic phenomena)", Ed.Academiei Române, Bucureşti, 1982
[2]. *Horia Gavrilă, Horia Chiriac, Arthur Yelon, Ionita Valentin*, "Magnetism tehnic şi aplicat(Technical and applied magnetism)", Editura Academiei Române, Bucureşti, 2000
[3] *M.Ignat, N.Galan,A.Dalea*, "Short Introduction on the magnetostrictive motor" Bulletin of Micro and Nanoelectrotechnologies, nr.1-2, 2015,pp. 29- 34.
→[4] J. M. Vranish, D. P. Naik, "Magnetostrictive Direct Drive Rotary Motor Development", NASA GoddardSpace Flight Center, Greenbelt, MD 20771;
[5] M. Ignat, G. Zarnescu, I. Puflea, Al. Catanescu, L.Paslaru, V. Stoica, "Actuatori electromagnetici", Ed.Electra, 2008, pp. 22-50;
→[6] M. Ignat, I.Ardelean, G. Zarnescu, S. Soltan, "Micro-actionari neconventionale", Ed. Electra, 2006,pp.22-54.
[7]. Zhi Li, Xiuyu Zhang, Guo-Ying Gu, *Member, IEEE,* Xinkai Chen, *Senior Member, IEEE*, and Chun-Yi Su, *Senior Member, IEEE,* A Comprehensive Dynamic Model for Magnetostrictive Actuators ConsideringDifferent Input Frequencies With Mechanical Loads, IEEE TRANSACTIONS ON INDUSTRIAL INFORMATICS, VOL. 12, NO. 3, JUNE, pp. 980 – 990, 2016.
[8]. J. S. Park , O. K. Oh , Y. W. Park, and N. M. Wereley, A Novel Concept and Proof of Magnetostrictive Motor , IEEE TRANSACTIONS ON MAGNETICS, VOL. 49, NO. 7, JULY 2013, pp. 3379 – 3382
[9]. F. Claeyssen, N. Lhermet, R. Letty, and P. Bouchilloux, "Design and construction of a resonant magnetostrictive motor," *IEEE Trans. Magn.*, vol. 32, pp. 4749-4751, 1996.
[10]. Z. Cao and J. Cai, "Design of a giant magnetostrictive motor driven by elliptical motion," *Sens. Actuat. A*, vol. 118, pp. 332-337, 2004.
[11]. N. Zhou, C. C. Blathcley, and C. C. Ibeh, "Design and construction of a novel rotary magnetostrictive motor," *Appl. Phys. J.*, vol. 105, pp.113-115, 2009.
[12]. L.G. Bujoreanu, Materiale inteligente, Editura Junimea, Jaşi, 2002.
[13] . http://tdvib.com/terfenol-d/
[14]. http://tdvib.com/galfenol/
[15] M. B. Moffett, "Characterization of Terfenol-D for magnetostrictive transducers," *J. Acoust. Soc. Amer.*, vol. 89, pp. 1448-1455, 1991.
[16]A. Arnau, *Piezoelectric Transducers and Applications*. New York:Springer-Verlag, 2004.
[17] F.T. Calkins, M.J. Dapino and A.B. Flatau, "Effect of prestress on the dynamic performance of a Terfenol-D transducer", Proceedings of SPIE Smart Structures and Materials 1997, Vol. 3041, pp. 293-304, San Diego, CA, March 1997.
[18] R. Kellog, A. Flatau, Aerospace Eng. & Eng., Mechanics, Iowa State University, IA50011, Blocked force investigation of a Terfenol-D transducer,1999 SPIE's Symposium on Smart Structures and Materials, paper # 3668-19.
[19]. O. Bottauscio, M. Chiampi, A. Lovisolo, P. E. Roccato, and M. Zucca, "Dynamic modelling and experimental analysis of Terfenol-D rods for magnetostrictive actuators," *J. Appl. Phys.*, vol. 103, 2008, 07F121/1-3.
[20]A. E. Clark, M. Wun-Fogle, and J. B. Restorff, and T. A. Lograsso, "Magnetostrictive properties of galfenol alloys under compressive stress," *Mater. Trans.*, vol. 43, no. 5, pp. 881-886, 2002.
[21]. J. Zhou, M. Huang, X. Wang, and W. Song, "Development of a magnetostrictive drive rotary motor driven by circular parallel movement," *Smart Mater. Struct.*, vol. 16, pp. 2063-2066, 2007.
[22]. S. Karunanidhi and M. Singaperumal, "Design, analysis and simulation of magnetostrictive actuator and its application to high dynamic servo valve," *Sens. Actuators A, Phys.*, vol. 157, no. 2, pp. 185-197, 2010
[23] R. R. Basantkumar, B. J. H. Stadler, W. P. Robbins and E. M. Summers, "Integration of Thin-Film Galfenol With MEMS Cantilevers for Magnetic Actuation," IEEE Transactions on Magnetics, vol. 42, no. 10, pp. 3102-3104, 2006.
[24]. A. E. Clark, J. B. Restorff, M. Wun-Fogle, T. A. Lograsso and D. L. Schlagel, "Magnetostrictive properties of body-centered cubic Fe-Ga and Fe-Ga-Al alloys.," IEEE Transactions on Magnetics, vol. 36, no. 5, pp. 3238-3240, 2000.

[25]. Olabi A.G., Grunwald A., "Design and application of magnetostrictive materials", ScienceDirect, Materials and Design, No. 29 (2), 2008, pp. 469-483, ISSN 0261-3069.
[26]. ***Cătănescu Alexandru-Laurenţiu*** **Acţionări neconvenţionale utilizând actuatori magnetostrictivi, *Teză de doctorat. C*onducător ştiinţific ,**prof. dr. ing. C**ezar Fluerașu, Bucuresti, 2014.**
[27]. S. C. Cao, B. Wang, J. Zheng, W. Huang, Y. Sun, and Q. Yang, "Modeling dynamic hysteresis for giant magnetostrictive actuator using hybrid genetic algorithm," *IEEE Trans. Magn.*, vol. 42, pp. 911-914, 2006
[28]. M. J. Sablik and D. C. Jiles, "Coupled magnetoelastic theory of magnetic and magnetostrictive hysteresis," *IEEE Trans. Magn.*, vol. 29, pp.2113-2123, 1993.
[29]. M. J. Dapino, R. C. Smith, and A. B. Flatau, "Structural magnetic strain model for magnetostrictive transducer," *IEEE Trans. Magn.*, vol. 36, no. 3, pp. 545-556, 2000.
[30]. R. C. Smith, M. J. Dapino, and S. Seelecke, "Free energy model for hysteresis in magnetostrictive transducers," *J. Appl. Phys.*, vol. 93, pp.458-466, 2003.
[42]. F. Claeyssen, N. Lhermet, R. Letty, and P. Bouchilloux, "Design and construction of a resonant magnetostrictive motor," *IEEE Trans. Magn.*, vol. 32, pp. 4749-4751, 1996.
[43]. H. Yoshioka, H. Shinno, and H. Sawano, "A newly developed rotary-linear motion platform with a giant magnetostrictive actuator," *CIRP Ann.-Manuf. Technol.*, vol. 62, no. 1, pp. 371-374, 2013.
[44]. F. Claeyssen, N. Lhermet, R. Le Letty, and P. Bouchilloux, "Actuators, transducers and motors based on giant magnetostrictive materials," *J. Alloys Compd.*, vol. 258, no. 1/2, pp. 61-73, Aug. 1997.
[45]. P. Campbell, *Permanent Magnet Materials and Their Applications*.New York: Cambridge Univ. Press, 1994.
[50]. *J.S. Park, O.K. Oh, Y.W.Park, N.M. Wereley*; "A Novel Concept and Proof of Magnetostrictive Motor", IEEE Transactions on Magnetics , vol. 49, NO 7 July, 2013, pp 3379 – 3382
[51] T. Akuta, "Rotational-type actuators with terfenol-D rods," in *Proc 3rd Actuator Conf.* , 1992, pp. 244-248.
[54]. **Alexandru Dalea,** Mircea Ignat, Sorin Deleanu, Mihai Iordache, Neculai Galan, "Optimal Operation of the Rotary Magnetostrictive Motor", Publisher: IEEE, IEEE Xplore, 2018 International Conference on Applied and Theoretical Electricity (ICATE), DOI: 10.1109/ICATE.2016.7754705, 978-1-5386-3806-4/18/$31.00 ©2018 IEEE, Page(s): 1 - 6.
[55].**. Alexandru Dalea**, Mircea Ignat, Sorin Deleanu, Mihai Iordache, Neculai Galan, "The Rotary Magnetostrictive Motor: a Promising Solution for Low Power Actuators, Annals of the University of Craiova, Electrical Engineering series, No. 42, Issue 2, 2018; ISSN 1842-4805, pp. 10 - 28.
[56].**. Alexandru Dalea**, Mircea Ignat, Mihai Iordache, Neculai Galan, „Rotary Magnetostrictive Motor", Proc. of the 12th International Conference on Electromechanical and Power Systems, SIELEM 2019, October 11-14, 2019, Chișinău Rep. MOLDOVA, IEEE Xplore, 978-1-4673-7488-0/15/$31.0 2015IEEE, **DOI:** 10.1109/SIELMEN.2017.8123295 , **Publisher:** IEEE, pp. 1-7 (in press).
[57]**. Alexandru Dalea**, Mircea Ignat, Sorin Deleanu, Mihai Iordache, Neculai Galan, „Consideraţii privind funcţionarea motorului magnetostrictiv rotativ", Proc. SME'16 Ediția a XII-a, București 9 noiembrie 2018 ISSN: 1843-5912, pe CD, pp. 61-72.
[58].Mircea Ignat, Alexandru Dalea, Neculai Galan, *INCDIE ICE CA,**UPB-Facultatea de Inginerie Electrica, **Incercarile preliminare ale unui motor magnetostrictiv**, SIMPOZIONUL DE MAŞINI ELECTRICE SME'15– 23 Octombrie, 2015.
[59]. Mircea Ignat, Alexandru Dalea, Neculai Galan, **Motor magnetostrictiv rotativ**, SIMPOZIONUL DE MAŞINI ELECTRICE SME'15–23 Octombrie, 2015
[60]. Mircea Ignat, Alexandru Dalea, Neculai Galan,INCDIE ICE CA,**UPB-Facultatea de Inginerie Electrica, **ASPECTE TEORETICE SI EXPERIMENTALE PRIVIND REGIMUL DINAMIC AL CONTACTULUI MECANIC LA MOTORUL MAGNETOSTRICTIV ROTATIV**, SIMPOZIONUL DE MAŞINI ELECTRICE SME'16 – 11 Noiembrie, 2016.
[61] D. Bushko, J. Goldie, "High Performance Magnetostrictive Actuators", IEEE AES Systems Magazine, November 1991, pp. 251-267;

[62]. Z. Cao and J. Cai, “Design of a giant magnetostrictive motor driven by elliptical motion,” *Sens. Actuat. A*, vol. 118, pp. 332-337, 2004.
[63]. Mircea IGNAT, **Alexandru-Laurentiu CATANESCU**, Ioan PUFLEA, „Applications of the Magnetostrictive Actuators in the Aerospace Structures”, International Conference of Aerospace Sciences “AEROSPATIAL 2010”**,** Bucharest, 20-21 October, 2010, Proceedings, Section 4. Materials and Structures, ISSN 2067-8622, pp.1-6.
[64] Nova[1], V. Havlicék[2], and I. Zemanék[2], “Dynamic hysteresis loops modeling by means of extended hyperbolic model”, pg.148, contributii lucrari:
[65] J. Takács, Mathematics of Hysteretic Phenomena. Berlin, Germany:Wiley, 2003.
[66] https://ro.scribd.com/doc/182116437/OLC45-docx
[67] https://ro.scribd.com/document/42586533/S235JR-sau-OL-37